

## REVIEW

# Structure and design of polymers for durable, stretchable organic electronics

Jonathan Onorato<sup>1</sup>, Viktoria Pakhnyuk<sup>2</sup> and Christine K Luscombe<sup>1,2</sup>

The field of stretchable electronics has recently gained significant interest from the academic community, with a focus on producing materials that demonstrate reliable electrical performance with improved response to mechanical deformation. This review highlights the recent progress in understanding the relationships between the mechanical behavior and electrical performance of such devices. Potential solutions can take the form of intrinsically elastic polymers, polymer semiconductor/elastomer blends and alternative engineering-oriented approaches, which are discussed herein. Trends and design strategies are beginning to manifest in this early stage of the stretchable electronics field. The development of stretchable electrical systems can provide unique applications of organic electronics.

*Polymer Journal* (2017) 49, 41–60; doi:10.1038/pj.2016.76; published online 7 September 2016

## INTRODUCTION

From the initial discovery of the semiconducting properties of doped polyacetylene (1) in 1977 (Figure 1),<sup>1</sup> great strides have been made to improve the lifetime<sup>2–6</sup> and electrical properties<sup>7–12</sup> of conjugated polymers in organic electronics, even having organic field-effect transistor materials surpass silicon.<sup>13</sup> Unlike inorganic semiconductors such as silicon, semiconducting polymers have the potential to be optically transparent,<sup>14</sup> rapidly and easily processable<sup>15</sup> and mechanically compliant, all of which can be potential advantages for organic electronics.<sup>16</sup> Mechanical compliance in particular allows the use of semiconducting polymers in unique electronics applications where stretchability is a key factor. This improved elasticity will translate into more durable systems even in more traditional applications, like photovoltaics, transistors, light-emitting diodes and sensors. Although some polymers are theoretically capable of high stretchability, many of the commonly used conjugated polymers are not. Recent studies investigating field-tested organic photovoltaic (OPV) devices found that the primary source for device failure was through mechanical failure.<sup>17,18</sup> Although similar trends have yet to be reported in other devices, there is still a clear advantage for other devices to have stretchability, as it opens up new applications for these devices, including conformal light-emitting diodes and electronic skin.<sup>19–21</sup>

The solubility and flexibility of polymers allows for devices to be processed by low-cost solution processing methods including reel-to-reel; however, this flexibility does not indicate elasticity.<sup>22</sup> Damage to these devices could even occur during processing. In the thin-film industry, it has been shown that improved mechanical properties are linked to higher production yield during mass production.<sup>23</sup> Flexibility relates to the ability of a material to be bent, such as rolling up a poster, whereas stretchability relates to the ability

to pull on a material, such as pulling on a rubber band. This distinction is described pictorially in Figure 2. The use of very thin (approx. 1  $\mu\text{m}$ ), flexible substrates such as polydimethylsiloxane (PDMS) allows for the device to be bent to a 1 cm radius while still producing elongation strains low enough to avoid cracking in most semiconducting polymers.<sup>24</sup> With that said, these devices will still fail if they are pulled in tension, and this distinction implies that tensile stress is the more relevant parameter to measure device durability than bending. Devices will be subjected to unpredictable and occasionally dramatic stresses during processing, thermal cycling, stretching and bending of the device under general use, thus materials with high elasticity are desirable to ensure the success of a range of organic electronic applications. Due to the inherent  $\pi$ -conjugation of organic conductors and the resultant stiffness, these materials are often very brittle when stretched. Improvements in mechanical properties directly relate to protection of the electrical properties of a thin film. Specifically, the higher the film's resistance to mechanical fatigue, the less conductivity loss with mechanical cycling.<sup>25</sup> Because of this, significant innovation is needed both from a chemical and engineering design perspective to develop inherently stretchable materials. The ideal polymeric system would exhibit high ductility and be able to maintain its maximum conductivity after numerous strain cycles on the material, allowing for the preservation of electrical properties under cyclic stresses.

This review will maintain as its primary focus the use of polymers as stretchable active layer materials in solar cells, and will also present information relevant to other stretchable electronics. This article's focus on stretchable solar cells is due to the existence of several reviews, which discuss stretchable systems for other applications,<sup>26</sup> such as organic field-effect transistors<sup>27</sup> and light-emitting diodes.<sup>28,29</sup> Previous reviews on mechanical properties of

<sup>1</sup>Materials Science and Engineering Department, University of Washington, Seattle, WA, USA and <sup>2</sup>Department of Chemistry, University of Washington, Seattle, WA, USA  
Correspondence: Professor CK Luscombe, Materials Science and Engineering Department, University of Washington, Roberts Hall, Seattle, WA 98195-2120, USA.  
E-mail: luscombe@uw.edu

Received 22 June 2016; revised 22 July 2016; accepted 23 July 2016; published online 7 September 2016

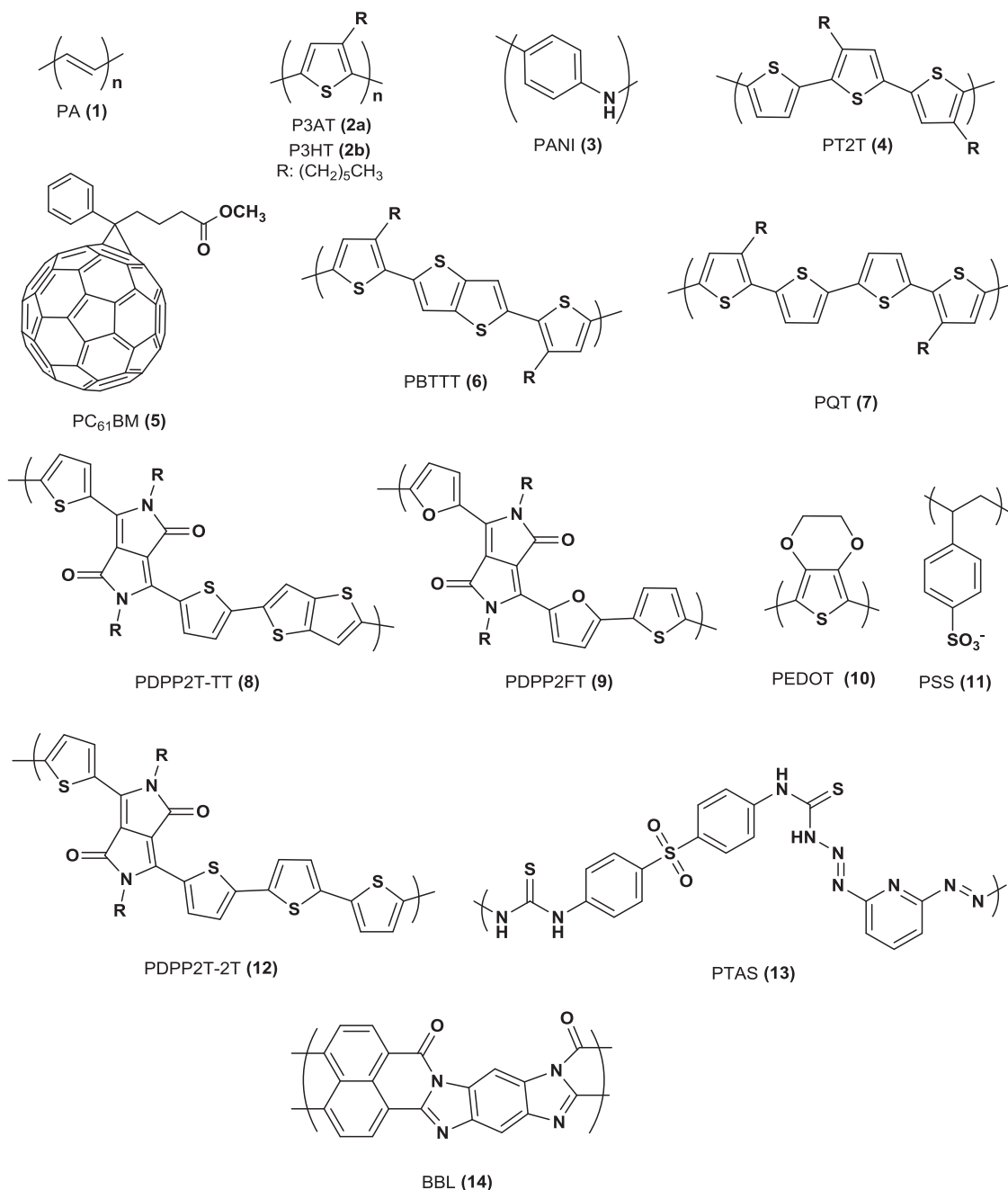


**Figure 1** Several semiconducting polymers that will be discussed throughout this article.

solar cells maintained as their primary focus the goal of presenting the value of stretchable materials, as well as their feasibility.<sup>30</sup> The present review instead presents specific levers for adjusting mechanical properties of conjugated polymers and copolymers, and provides explanations for the mechanisms of these changes. We provide general background for understanding electrical and mechanical properties, then discuss trends between the two in conjugated homopolymers, copolymers and polymer blends. Alternative designs to mitigate strain-related damage to conducting segments in organic electronics are presented, and a proposal for a standardized set of measurement techniques for stretchable devices is proposed.

## CHARACTERIZATION METHODS

Outlined here are common figures of merit and their measurement techniques used to quantify electrical and mechanical properties of materials. These methods are presented to illustrate key property test methods, creating a standardized characterization method set to provide for clear comparisons of material properties between separate studies. Improved performances of materials are summarized in Table 1 with desirable electrical properties, which would have higher conductivity or lower resistance, greater charge mobility and increased efficiency. Desirable mechanical properties would have a reduced Young's modulus (or simply modulus), higher tensile strength, increased elongation at break and greater crack-onset strain.

### Electrical properties

**Conductivity.** The simplest method to collect a material's basic electrical properties is with commercially available two-point or four-point probes, which determine conductivity and resistance.<sup>31</sup> The four probe method is preferred because of the high variability associated with two-point probes.<sup>32,33</sup> Except where otherwise stated, this technique was used to measure conductivity or resistance in the reviewed literature.

**Charge mobility.** Another component of electrical properties is the charge mobility, which can be evaluated in a number of ways including the use of time of flight, space-charge limited current and flash photolysis time-resolved microwave conductivity.<sup>34–40</sup> A common tool for measurement utilized in the reviewed literature is the field-effect transistor. A typical architecture is illustrated in Figure 3 with top-contact source and drain on the conducting active layer, and the dielectric insulating the bottom gate. Though transistors require fabrication, additional figures of merit are gained compared with the probing method, including threshold voltage and current on/off ratio.<sup>41</sup>

**Power conversion efficiency.** The device currently of high interest to the scientific community, and a highlight of this review is the solar cell. OPVs are commonly fabricated in the bulk heterojunction (BHJ) architecture, where an active layer blend of donor and acceptor molecules lies between electrodes illustrated in Figure 4a. Standardized parameters,<sup>42,43</sup> namely the FF (fill factor), which measures the quality of a solar cell, and the power conversion efficiency (PCE), are determined from plots of current density vs voltage, or  $J$ - $V$  curves (Figure 4b; equations (1 and 2)).

$$FF = \frac{P_{Max}}{P_{Theo}} = \frac{J_{Max}V_{Max}}{J_{SC}V_{OC}} \quad (1)$$

The maximum power,  $P_{Max}$ , is defined as the largest rectangular area under the curve, and the theoretical power,  $P_{Theo}$  is a product of

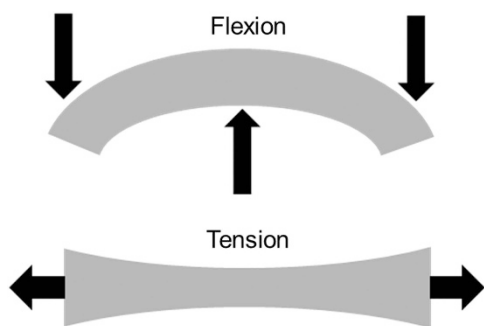


**Figure 2** Schematic illustration of stretching and flexing in a thin-film architecture.

**Table 1** Improved electrical and mechanical properties are defined by the relative quantities of discussed parameters

Improved electrical properties		Improved mechanical properties	
↑	Conductivity	↑	Elongation at break
↑	Charge mobility	↑	Tensile strength
↑	Power conversion efficiency	↑	Crack-onset strain
↓	Resistance	↓	Modulus

the short circuit current,  $J_{SC}$ , and open-circuit voltage,  $V_{OC}$ .

$$PCE = \frac{P_{Max}}{P_{in}} \quad (2)$$

The power conversion efficiency, or simply efficiency, is the ratio of electrical power output,  $P_{Max}$ , to solar power input,  $P_{in}$ , and the basis for comparing solar cell performance.

### Mechanical properties

**Tensile testing.** Tensile testing is the industry standard methodology for understanding the mechanical properties of a bulk material.<sup>44</sup> This testing methodology allows the user to determine key material properties such as modulus, yield and maximum strain, toughness and tensile strength. A set of typical stress-strain curves, the result of a tensile test, can be seen in Figure 5, depicting the behavior of brittle, plastic and elastomeric material responses. The modulus is the slope of the initial linear regime, and is qualitatively the stiffness of the material. Several important limits are worth defining. Notably, the maximum stress the material can withstand before being permanently damaged is the yield stress. Unfortunately, this parameter, while critical to interpreting the material's ability to handle stress without damage, is rarely measured for semiconducting polymers. Much of the early testing of mechanical properties of bulk semiconducting polymers utilized this methodology.<sup>45–47</sup> Because of the difficulty of preparing free-standing nanoscale films of the semiconducting polymer, this method is usually reserved for bulk material properties. With that said, the results from a tensile test are often used as a benchmark to quantify material properties.

**Thin-film buckling test.** Thin-film buckling is a relatively new testing method that can be used to measure the modulus of a very thin layer of material. The method affixes the tested film on a pre-strained substrate, which is then allowed to relax to its original length. This process results in the whole material forming sinusoidal waves, which can be seen in Figure 6. The wavelength of this sinusoidal feature is dependent upon the difference of moduli and can be used to extract the modulus, as per equation (3).<sup>48</sup>

$$E_f = 3E_s \left( \frac{1 - \nu_f^2}{1 - \nu_s^2} \right) \left( \frac{\lambda_b}{2\pi d_f} \right)^3 \quad (3)$$

The buckling wavelength method equation.

Here,  $E_f$  is the modulus of the film and  $E_s$  is the modulus of the substrate. Likewise,  $\nu_f$  is the Poisson's ratio of the film and  $\nu_s$  is of the substrate.  $\lambda_b$  is the buckling wavelength and  $d_f$  is the thickness of the film.

The sinusoidal pattern was first observed in thin films of metal on stretchable substrates, and again in a surface-oxidized stretchable polymer.<sup>49,50</sup> It is produced by a buckling phenomenon, resulting from a strong compressive force with release of the pre-strain in the elastic substrate.<sup>51</sup> There is no dependence on film thickness over the ranges expected in nanoscale films, allowing for films of any thickness

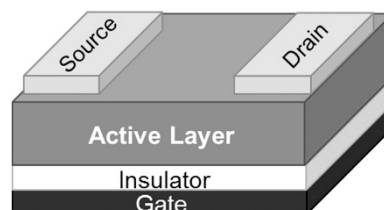


**Figure 3** Architecture of a top-contact bottom-gate field-effect transistor.

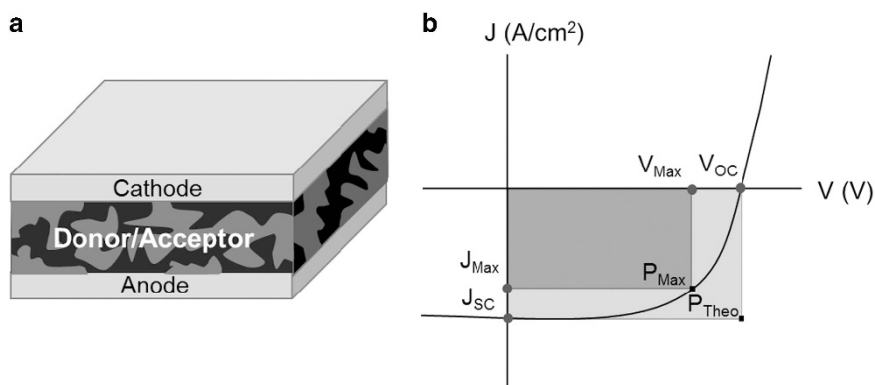


**Figure 4** (a) Simple bulk heterojunction architecture for organic solar cells. (b) Representative photovoltaic  $J$ - $V$  curve and its parameters.

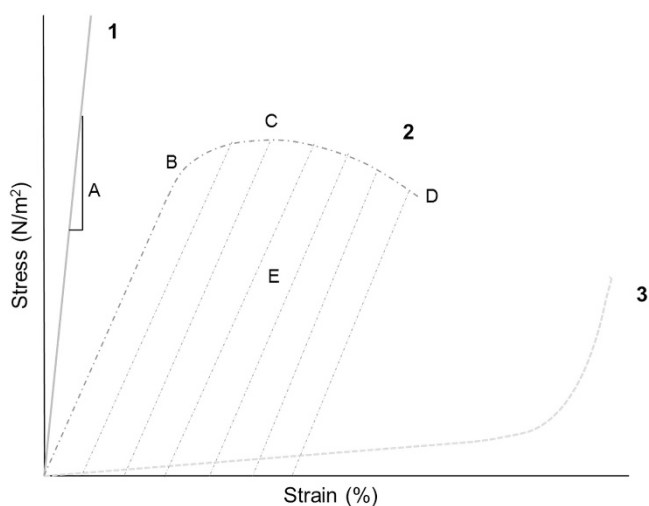


**Figure 5** A pictorial representation of a typical stress-strain curve for (1) a brittle material, (2) a plastic material and (3) an elastomer. Several key features are noted on this diagram the: (A) modulus; (B) yield point which gives both yield strength and strain at yield; (C) tensile strength is the maximum stress; (D) elongation at break; and (E) toughness, which is the shaded area under the curve.

to be measured.<sup>50</sup> This method can be used to determine the modulus of many types of thin films, including semiconducting polymers.<sup>52</sup>

**Crack-onset strain.** The crack-onset strain method is a commonly used technique for measuring the maximum plane strain for nanoscale thin films.<sup>53,54</sup> The thin film to be measured is deposited on a stretchable substrate to allow the film to support its own weight during testing. The film is then stretched, incrementally increasing the strain. Optical images are taken at each of these incremental strains to observe any crack formation.<sup>53</sup> The reported crack-onset strain is the strain at which the first crack is observed using the optical micrographs.<sup>53</sup>

### MECHANICAL FAILURE MODES IN POLYMER SOLAR CELLS

In designing stretchable solar cells, it is important to understand the main mechanical modes of failure in multilayer film systems, like those used in polymer solar cells. This gives insight into how best to approach a solution to the mechanical degradation observed. Mechanical failure of multilayer systems is separated into failure at the interfaces or in the bulk.<sup>55</sup> At this time, the majority of studies

highlight the changes in electrical properties but do not illustrate the mechanical mechanism of failure. Understanding the mechanism by which these films fail can inform methods for how to improve the mechanical response, as will be discussed in this section. Because of this, it is important that future studies investigate these mechanisms and use them to produce optimized multilayer films.

#### Adhesive failure

One of the mechanisms by which multilayer films experience catastrophic failure is through failure at the interface between two layers, or adhesive failure. Adhesive failure qualitatively occurs when the tensile strength of the interface is lower than the tensile strength of either bulk material. Adhesive failure is worsened by poor interfacial compatibility,<sup>56</sup> and a lack of surface interdiffusion,<sup>57</sup> among other factors.<sup>58-60</sup>

#### Cohesive failure

The other mechanism of catastrophic failure is cohesive failure, which occurs in the bulk of one of the materials in the multilayer film. The film layer with the lowest tensile strength will break first, effectively limiting the strength of the multilayer film system to that of the weakest layer. Ultimately, cohesive failure is a best-case scenario, as it indicates interlayer compatibility and that the limitations of the multilayer film are inherent to the materials used. This is especially critical for polymer blends, where poor compatibility or blending can cause the properties of the bulk material to degrade significantly.<sup>60</sup>

#### Non-catastrophic failure mechanisms

The aforementioned failure mechanisms represent catastrophic failure mechanisms, but there are many non-catastrophic mechanisms that degrade either the mechanical or electrical properties of a device. Microscale cracks, and strain-induced crystallinity changes are particularly important in polymer solar cells. Microcracks form around structural defects in the material, including impurities and microvoids.<sup>61</sup> These microcracks result in an increase in intrinsic device resistance and reducing the short circuit current.<sup>62</sup> Images of microcracks, and the effects of material stretchability can be seen in Figure 7. Interestingly, when the strain is released from a plastically deformed device, the device buckles and compresses. The device can then be elongated back to the previous strain values without further damage.<sup>24</sup> Mechanical strain also changes crystallinity through strain alignment. It is well known that drawing polymer fibers or films can increase crystallinity.<sup>63,64</sup> Likewise, applying stresses to a polymer solar cell can allow for rearrangement of polymer chains in the film.<sup>20</sup> Early studies of semiconducting polymers took advantage of this effect,

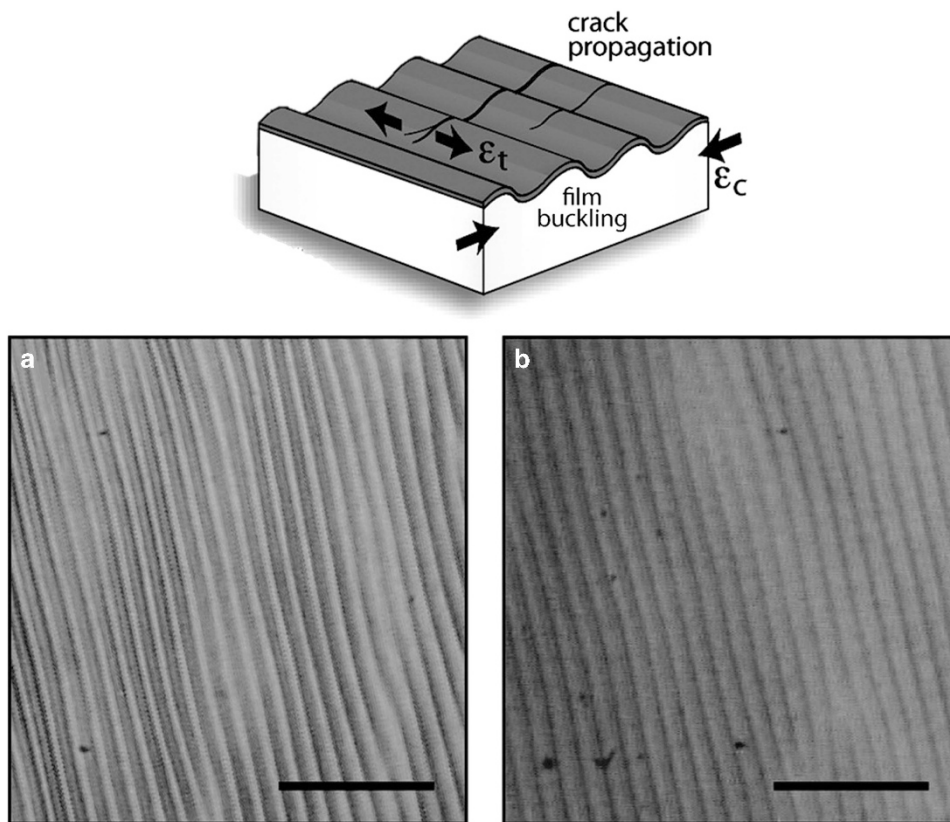


**Figure 6** The top figure depicts a cartoon version of this buckling phenomenon for added clarity, illustrating the sinusoidal nature of the buckling pattern. The scale bar on the bottom pictures is 100  $\mu\text{m}$ . The buckling wavelength shown in the optical micrograph is directly proportional to the modulus of the material. The material PBTTT (**b**) shows a larger wavelength, indicating that it is a more rigid polymer than P3HT (**a**). Reproduced from O'Connor *et al.* with permission from the American Chemical Society.<sup>69</sup>

drawing polymer films to orient chains and increase crystallinity, thereby increasing the modulus.<sup>1,65</sup>

### MECHANICAL PROPERTIES OF HOMOPOLYMERS AND ALTERNATING COPOLYMERS

This section focuses on intrinsic elastic properties of different semiconductor homopolymers and alternating copolymers as active layer materials for polymer solar cells. Several reviews discussing the design and fabrication of stretchable and highly conductive electrode materials already exist.<sup>66–68</sup> It is commonly understood that in many cases the device efficiency increases with the modulus of the BHJ material.<sup>69</sup> This increasing modulus results in brittle devices with severe property degradation even with minimal elongation. Beyond modulus, it is well known that both the morphology and crystallinity have a strong part in the device efficiency in polymer solar cells, and that there is significant interplay between the two.<sup>11,70</sup> It is widely acknowledged that the optimal domain size is 20 nm for each phase; larger sizes lead to increased exciton recombination, and smaller sizes reduce the interfacial area for charge separation.<sup>71</sup> This intermixed, small domain system is ideal for a high PCE, but may not necessarily be optimal for mechanical properties. There is a clear link between morphology, crystallinity and mechanical properties of a BHJ, but drawing trends between these changes and the mechanical properties is difficult due to the complexity of such systems.<sup>72–75</sup> Recent studies have investigated methods for improving extensibility; certain levers such as adjusting the crystallinity, morphology and changing chemical structure are presented here, and a theoretical framework for

understanding these modifications is outlined. The modulus and charge mobility of several polymers, along with PCBM, are plotted in Figure 8 to illustrate the general state of the field and the relative properties of these polymers.

#### Effect of alkyl side chains

This segment highlights the effects of alkyl side chains on the mechanical properties of conjugated polymers, but does not discuss the other major effects that these changes can have. For broader context on the effects of changing side chains, the authors recommend an excellent review.<sup>76</sup> The most commonly studied model for tuning the mechanical properties of a polymer through side-chain modification of poly(3-alkylthiophene) (P3AT) (**2a**), with the most common variant being poly(3-hexylthiophene) (P3HT) (**2b**), an efficient but brittle polymer that has a crack-onset strain of only 9%.<sup>76,77</sup> By increasing the length of the side chain to an octyl group, this strain can be improved to 65%.<sup>78</sup> This is largely attributed to a reduction in glass transition temperature,  $T_g$ .<sup>69</sup> This extended chain disrupts crystallization, which also has the effect of reducing charge carrier mobility.<sup>79</sup> As such devices made from poly(3-octylthiophene) (P3OT) have very low PCE of only 0.68%, in spite of chemical and band gap similarities to P3HT.<sup>80,81</sup> Blends and copolymers of P3HT (**2b**) and P3OT, as well as pure poly(3-heptylthiophene) (P3HpT), were investigated to optimize between the high charge mobility of P3HT (**2b**) and the extensibility of P3OT. P3HpT produced the best balance, ultimately maintaining the high crystallinity of P3HT (**2b**), while having a  $T_g$  lower than room temperature.<sup>82</sup> When mixed with



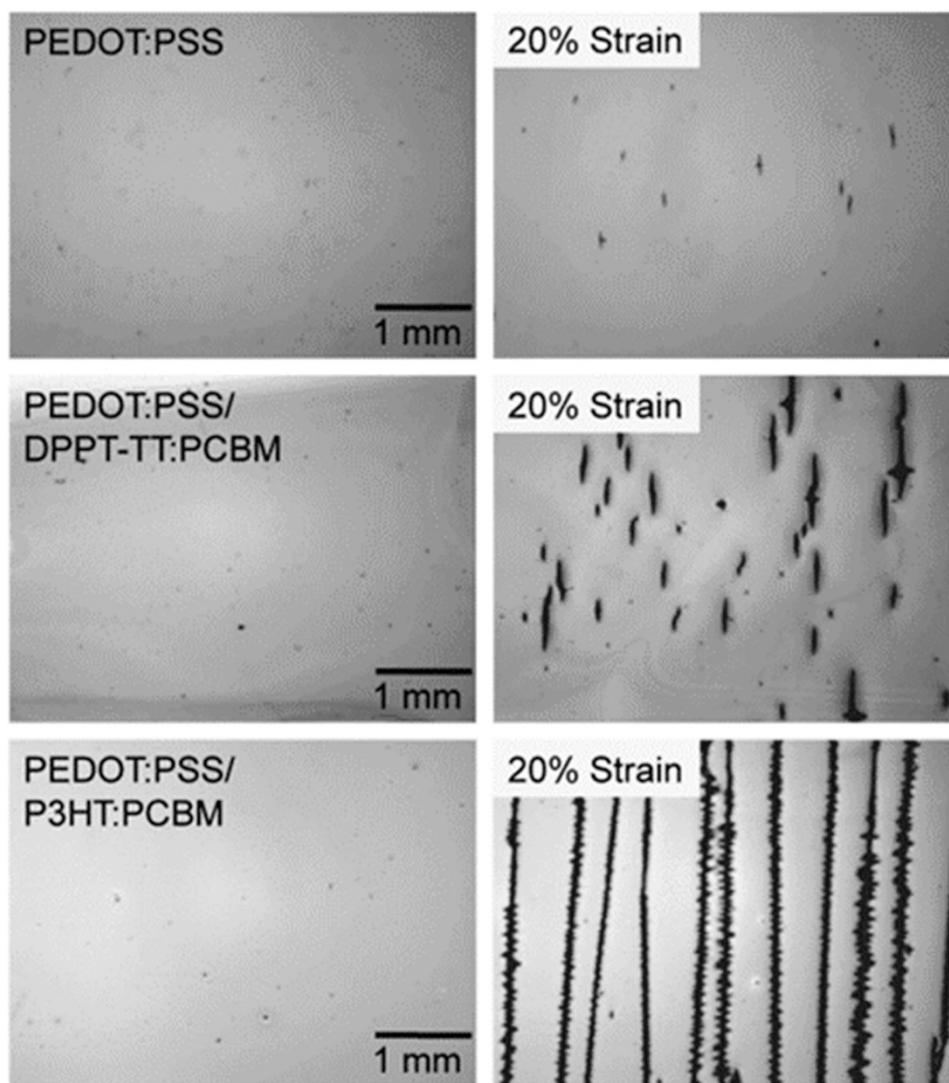


**Figure 7** Evolution of microscale cracks in the bulk heterojunction (BHJ) active layer material. Note that the stiffer P3HT:PCBM composite showed greater damage to the material with equivalent strain. Reproduced from Lipomi *et al.*<sup>24</sup> with permission from Elsevier.

PCBM (5), the anti-plasticizing effects of PCBM (5) result in a maximum elongation of only 4%, compared with a P3OT blend that retains 45% elongation.<sup>53</sup> Side chain branching is another powerful tool that disrupts crystallinity to a greater extent than linear chains, with minimal effects on the morphology.<sup>83,84</sup> For example, poly(3-(2'-ethyl)hexylthiophene) (P3EHT) was investigated and compared against P3HT (2b) and poly(3-dodecylthiophene) (P3DDT). P3EHT had significantly lower melting temperature ( $T_m$ ) and charge carrier mobility compared with P3HT (2b) and P3DDT, implying that the use of branching side chains may provide even more significant effects in lowering modulus, though at the cost of charge mobility.<sup>83</sup> The effect of the alkyl side chain on the mechanical properties in P3AT (2) seems to be largely dependent on  $T_g$  changes, as well as a decrease in percentage of carbon atoms along the main chain backbone and can be controlled by rational design.<sup>51</sup> In most cases, the decrease in  $T_g$  is also accompanied by decreases in the device efficiency, an effect which leads to the aforementioned belief that mechanical properties and efficiency are directly connected.

#### PCBM embrittlement and side chain spacing effects

When PCBM (5) is mixed into the BHJ blend, two potential pathways it could take are to form its own distinct crystalline domains, or intercalate into the blended polymer's structure and co-crystallize, though other possibilities exist. In PCBM (5)-containing films, domain size decreases lead to a decreasing modulus. The rigid acceptor phase also has a significant ordering effect on the BHJ, which is the origin of its anti-plasticization effects.<sup>85</sup> This is because large PCBM (5) domains lead to increased embrittlement due to the sharp boundaries between each crystallite.<sup>75,84,86</sup> Outside of ordering, the BHJ can co-crystallize.<sup>87–89</sup> This co-crystallized material has an increased stiffness as compared with a non-intercalated blend.<sup>23</sup> This effect can be investigated by comparing a series of thiophenes with increasing spacing, from P3AT (2a) to PT2T (4), PBTtT (6) and PQT (7). P3HT does not allow for intercalation due to the narrow spacing between alkyl side chains, although the addition of PCBM still embrittles the blend as previously mentioned. Pure PT2T (4) is known to be mechanically stiff with a modulus of 1.1 GPa, a value that is similar to that of P3HT at 1.3 GPa.<sup>90–93</sup> However, on addition of PCBM (5), PT2T (4) shows a significant change in modulus (1.6 GPa)

and poor efficiency (PCE=0.28%). This effect is due to the intercalation of PCBM (5) in PT2T (4) (Figure 9), embrittling the blend and hindering the formation of independent crystalline domains of PT2T (4) and PCBM (5) for efficient charge transport.<sup>83</sup> This effect is also seen with larger spacing, such as PBTTT (6),<sup>69,94,95</sup> and PQT (7).<sup>89</sup> It is important to note that this is dependent on the side chains as well; long, branching side chains can block intercalation in PBTTT (6), limiting these effects.<sup>87</sup> Because these BHJ blends co-crystallize, continuous charge transport pathways do not exist when loaded at a 1:1 polymer:PCBM (5) ratio. These pathways can be regenerated with excess loading of PCBM. If the PQT (7)

was loaded at 1:4 ratio of PQT (7):PCBM (5), charge transport pathways were formed and PCE was dramatically improved (0.28% at 1:1, 1.63% at 1:4).<sup>23</sup> Likewise for PBTTT (6) (0.25% at 1:1, 2.51% at 1:4).<sup>89</sup> The downside is that adding significant amounts of PCBM (5) to the blend results in a highly brittle BHJ blend, regardless of the polymer it is blended with, resulting in decreased cohesion across every polymer.<sup>23</sup> Further investigation into even greater spacing between chains, as well as the effect of the length of the alkyl chains in conjunction with changing the spacing between chains would be valuable in understanding side-chain-related modulus modifications.

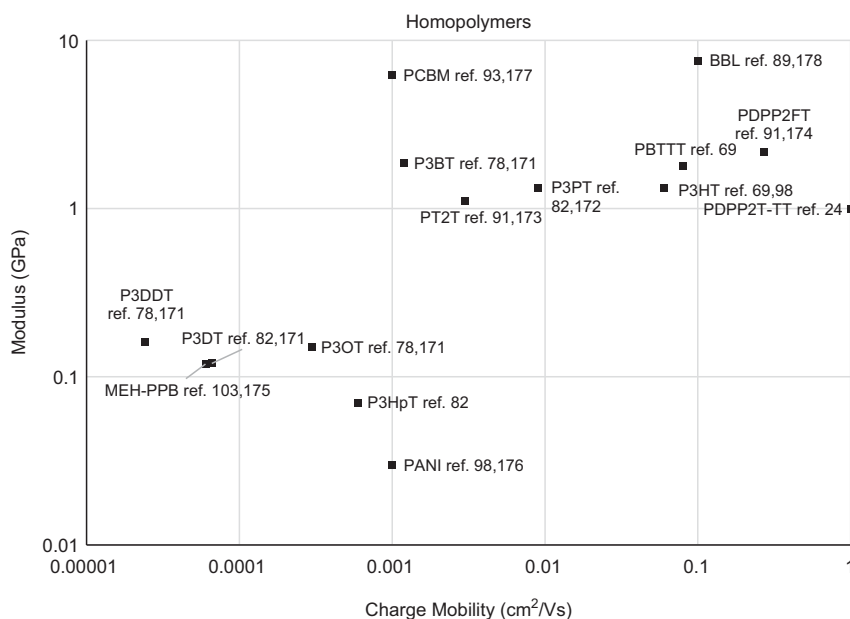


**Figure 8** A chart comparing charge mobility and modulus for a large variety of polymeric materials. The best materials would be those located towards the bottom right corner of the chart. The citations indicate first the mechanical property source, and second the electrical property source. MEH-PPV, poly[2-methoxy-5-(2-ethylhexyloxy)-1,4-phenylenevinylene]; PANI, polyaniline.

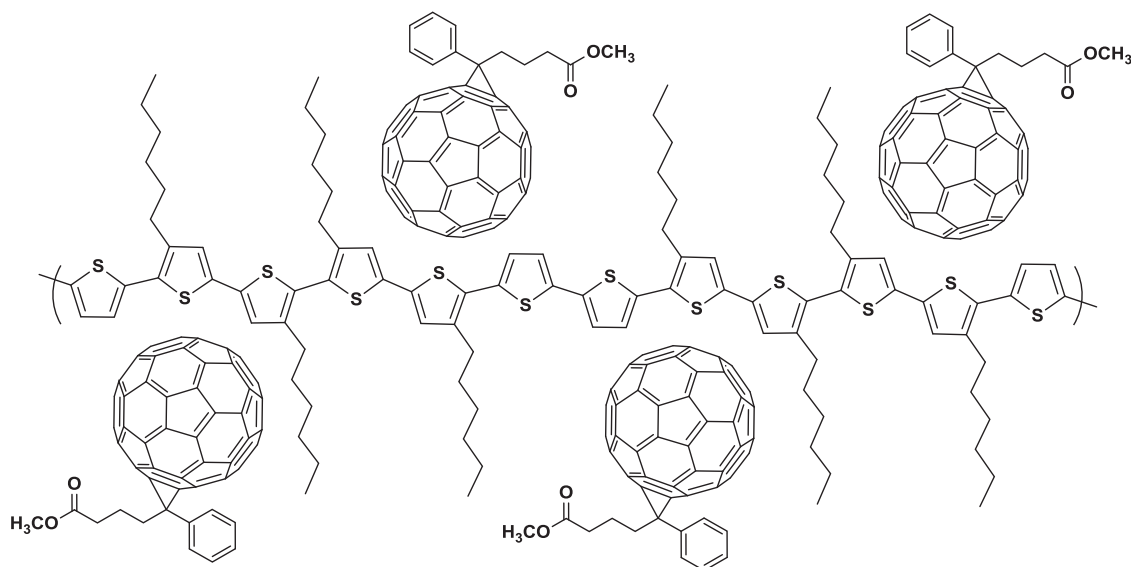


**Figure 9** Intercalated system of 5, the narrowest spacing allowing for intercalation in thiophene systems. Other thiophenes with greater alkyl chain spacing (notably 6 and 7) also demonstrate similar intercalation. P3HT, due to its narrow alkyl chain spacing, does not allow for PCBM intercalation.

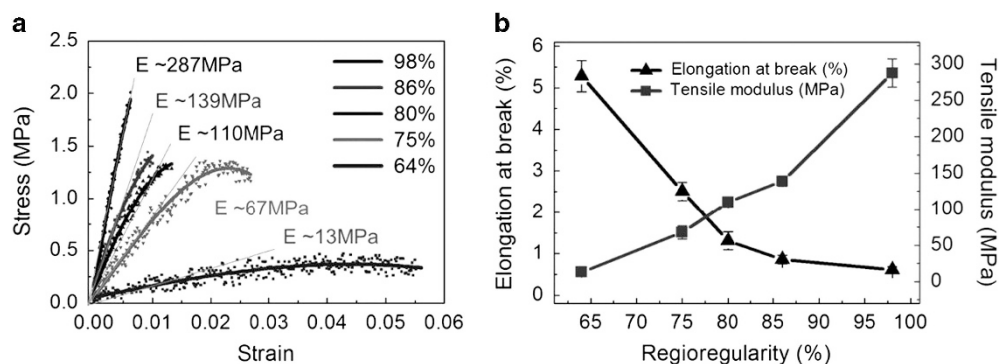


**Figure 10** The effect of changing regioregularity on a series of P3HT:PCBM composites. Stress-strain curves are shown in (a) illustrating the evolution of mechanical stress with strain. (b) Highlights the tensile modulus and elongation at break changes with regioregularity. Reproduced from Kim *et al.* with permission from American Chemical Society.<sup>107</sup>

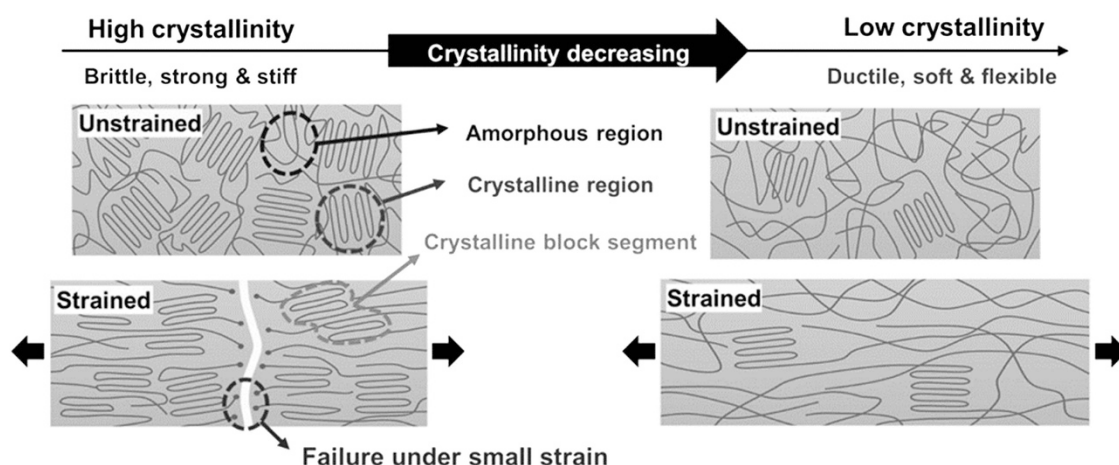


**Figure 11** The crystallite origin of the improvement in the stretchability of highly crystalline and low crystalline P3HT films. Reproduced from Kim *et al.* with permission from American Chemical Society.<sup>107</sup>

### Effect of fused vs free conjugated systems

In non-conjugated polymers, the stiffness of the polymer chain can be correlated to the molecular structure. Higher content of fused rings directly results in higher modulus, whereas inserting flexible spacer groups reduces the modulus.<sup>96</sup> Introducing kinks into the chain, such as with a *meta* linked benzene ring, can also lower the modulus.<sup>96</sup> It is reasonable to assume that these properties can be extended to semiconducting polymers and indeed a recent comprehensive study of donor-acceptor copolymers has confirmed that this trend is generally true.<sup>97</sup> Interestingly, morphological effects can sometimes overpower the changes due to these effects.<sup>97</sup> A system of various fused and non-fused thiophenes exhibit a clear trend; the greater the content of fused rings, the higher the modulus (notably PT2T (4) and PBT3T (6)).<sup>69,91,98</sup> This trend is also evident from PDPP2T-2T (12) and PDPP2T-TT (8). The non-fused thiophene ring allows for greater freedom of movement, resulting in a lower modulus for PDPP2T-2T (12) (0.74 GPa) than for PDPP2T-TT (8) (0.99 GPa).<sup>24</sup> Another example of this stiffening trend comes from ladder polymers such as BBL (14), a rigid polymer containing six fused rings, which has a modulus of 7.58 GPa.<sup>99</sup> Further studies must be performed on side chain modification in non-P3AT systems, and the variation between conjugated rings (furans, thiophenes, benzene, among other more complicated architectures) to fully understand the effects of fused rings on the mechanical properties of a BHJ active layer.

### Polymer organization and length

Other elements of a polymer can have an impact on the extensibility of a BHJ film. Increasing molecular weight can impact mechanical behavior, increasing toughness, although this effect saturates above a certain molecular weight.<sup>100</sup> This trend is also seen in semiconducting polymers, and has the added benefit of improving electrical performance in most systems as well.<sup>101,102</sup> This mechanical toughening arises from the increasing incidence of entanglement of chains with increasing molecular weight. These entanglements act as physical crosslinks, adding energetic barriers to moving chains.<sup>103</sup> In addition to the entanglements, increasing molecular weight can act to increase interconnects between polymer crystallites. As the polymer chains get longer, they will be incorporated into more than one crystal, forming interconnections. Increasing these interconnections is a way to improve both charge transport and mechanical properties. This occurs because these interconnections provide charge transfer pathways between crystal domains and also act as structural reinforcement by providing attachment points between the individual crystallites.

It has been shown in many cases that increasing the regioregularity (RR) of a polymer can increase its PCE.<sup>104-106</sup> Changing the RR also provides a strong mechanism by which to adjust the mechanical properties.<sup>107</sup> Specifically, going from a 98% RR P3HT to a 64% RR P3HT decreases the modulus from 287 to 13 MPa, and the maximum elongation from 0.5 to 5.5%, shown in Figure 10.<sup>107</sup> This change in RR also coincided with significant change in polymer molecular



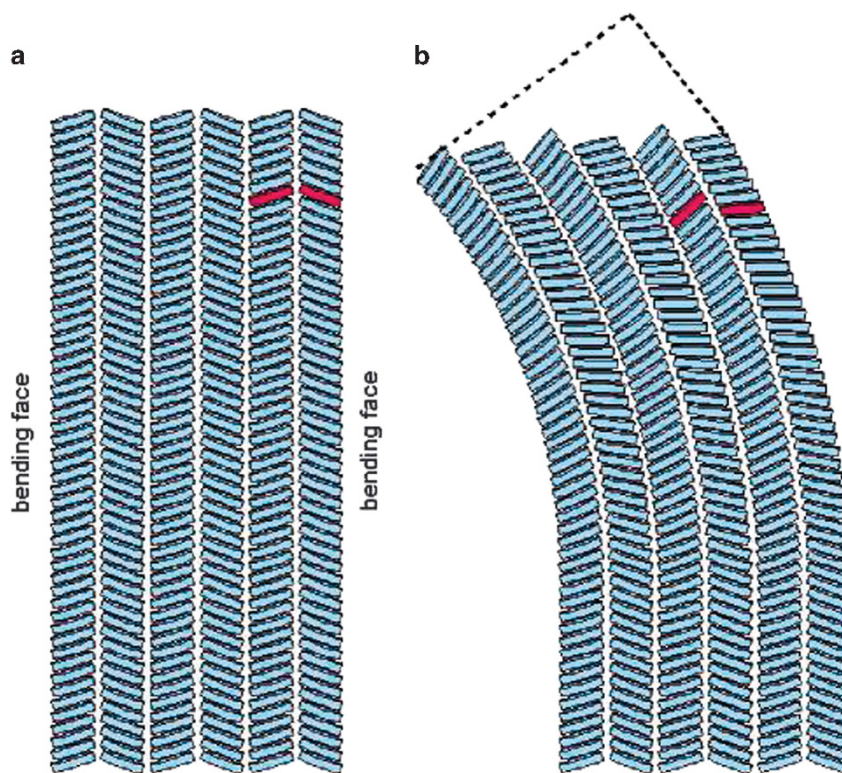


**Figure 12** (a) Depicts a schematic of an organic crystal with strong interactions in two-dimensional (2D), and weak interaction in the other (The white gap). (b) As shown, the crystal is able to flex by stretching along the weaker axis, sacrificing the weak interaction to maintain the strong 2D interactions. Reproduced from Reddy *et al.*<sup>109</sup> with permission from the American Chemical Society.

weight, from  $20.3 \text{ kg mol}^{-1}$  to  $9.2 \text{ kg mol}^{-1}$ .<sup>107</sup> Further studies should be performed to control for molecular weight to conclusively determine the effect of RR.

#### Percent crystallinity and crystallite rigidity

As percent crystallinity increases, so does the modulus, a trend generally true for all polymers. A pictorial depiction of the molecular basis for this effect is shown in Figure 11. The crystalline regions do not allow the amorphous region to extend, nor do the crystallites themselves allow for extension, and so the material cracks. In a lower crystallinity material, the amorphous regions can extend from a coiled structure into a linear structure, thereby providing a mechanism to allow for strain. In addition to simply changing the amount of crystallite, molecular design can be used to modify the molecular stretchability of a crystallite. Different strength of interaction in different directions can result in highly variable crystal mechanical properties, even with relatively similar chemical structures. Crystals can be deformable if weak intermolecular interactions exist in a direction nearly perpendicular to strong intermolecular interaction directions, schematically shown in Figure 12.<sup>108,109</sup> If the crystal has equivalent interactions in all three dimensions, it remains a brittle solid, even at temperatures approaching its melting point.<sup>108</sup> Note that the absolute magnitude of these interactions is not important; only the relative differences impact final mechanical properties.<sup>109</sup> If an appropriate consideration is taken for this during design of the photovoltaic polymer, then highly crystalline but deformable materials could be formed.

#### BLOCK AND RANDOM COPOLYMERS

For the purposes of this review, alternating copolymers are covered under 'homopolymers.' This section will focus on block and random copolymer active layer materials. Only limited studies into the mechanical properties of different copolymer systems have been performed, but the results therein indicate that copolymer systems may produce good compromises between mechanical properties and device performance. The combination of multiple polymers allows for a tuning of the properties of the final device by either altering the properties of the individual components, or by controlling the morphology, both of which can be advantageous for stretchable systems.<sup>110</sup>

##### Block copolymers

Block copolymers represent unique solutions to the problem of balancing the electrical and mechanical requirements of stretchable solar cells. When two chemically different polymers are used to synthesize a single block copolymer, the material tends to aggregate into phases that are rich in one segment or the other owing to a lack of polymer–polymer solubility. This phase separation results in a material that shows some properties of each material. Because of this segregation in copolymers of elastomers with semiconducting polymers, the copolymer retains a measure of its semiconducting ability, as well as gains some degree of elasticity.<sup>111</sup>

The first example of such a material, a P3HT (**2b**)-*b*-polyethylene (PE) copolymer reached a maximum strain of 660% with a composition of 10/90% P3HT (**2b**)-*b*-PE.<sup>112</sup> This copolymer also exhibited impressive conduction properties. The copolymer with only 10 wt% P3HT (**2b**) resulted in a field-effect transistor charge mobility of

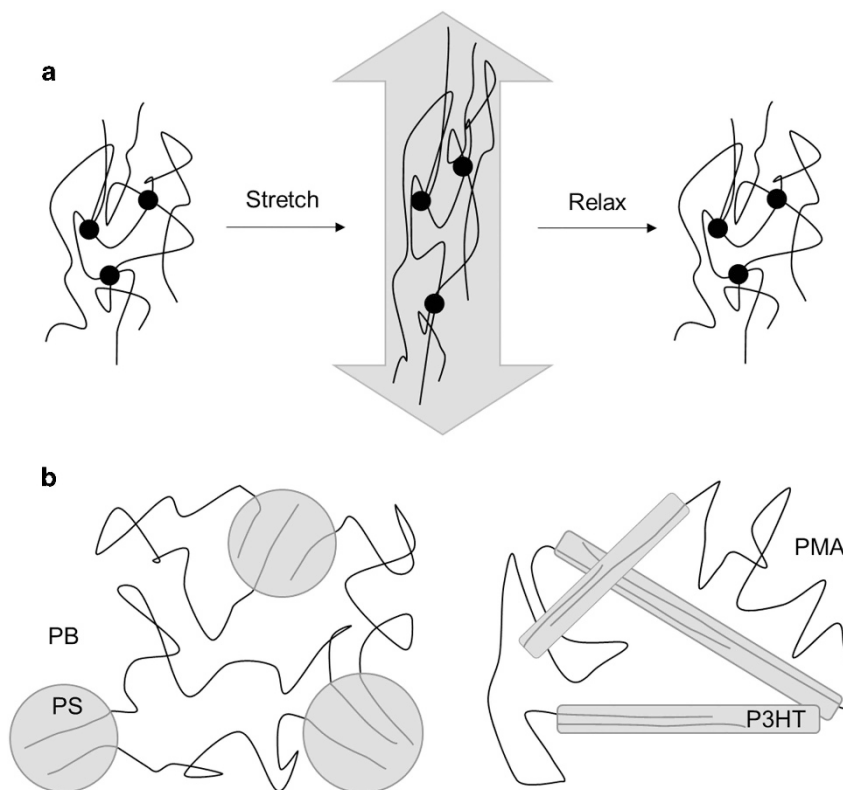


**Figure 13** (a) Schematic diagram of a thermoplastic elastomer (TPE). Black circles represent non-covalent crosslinking sites which prevent polymer chains from moving past one another and act as fixed points around which the polymer returns upon release from applied stress. Polymer chains around the black circles are highly coiled when there is no applied stress but uncoil when tension is applied. (b) Analogous to the common TPE poly(styrene-*b*-butadiene-*b*-styrene), a triblock copolymer of P3HT and PMA is illustrated to have a similar morphological mechanism for elasticity. Phase-segregated domains of hard (gray) and soft segments are formed due to the presence of a rigid block (polystyrene or P3HT) and coiled block (polybutadiene or PMA).

$2 \times 10^{-2} \text{ cm}^2 \text{ V}^{-1} \text{ s}^{-1}$ , whereas systems with 35 wt% P3HT (**2b**) showed mobilities approaching those of pure P3HT.<sup>112</sup> This results from the low percolation threshold, or the minimum concentration to achieve a continuous interconnecting pathway for charge transport, in the P3HT material when either blended or copolymerized with a polymer that crystallizes. These systems need only 10% P3HT to form co-continuous domains, a trend also observed in other P3HT copolymer systems.<sup>112,113</sup> It is important that the insulating polymer that is used in the copolymer is also semicrystalline, otherwise the percolation pathways can be significantly affected. An example of this comes in another system, where P3HT (**2b**) was copolymerized with poly(methyl methacrylate) (PMMA), an amorphous polymer, only resulting in good mobility with 40% P3HT (**2b**), illustrating the significant changes due to the crystallinity of the copolymer.<sup>111</sup> The crystallization of this system also has a significant role in the performance. For example, if P3HT (**2b**)-*b*-PE is deposited such that PE domains form first, the PE can restrict the crystallization of P3HT (**2b**), completely suppressing its transport properties. In that same system, allowing the P3HT (**2b**) to crystallize first resulted in distinct crystalline domains for both P3HT (**2b**) and PE. This result is a charge mobility of over four orders of magnitude larger, to  $0.02 \text{ cm}^2 \text{ V}^{-1} \text{ s}^{-1}$ , nearly identical to P3HT (**2b**).<sup>112</sup>

As the insulator component of the copolymer is not contributing to light absorption in most of these copolymer systems, it is likely that reduced absorption in the active layer would be a significant factor in reducing the short circuit current in these blends. As such, it would be advantageous to investigate systems only comprised of conjugated, absorptive polymers. As mentioned earlier, P3OT has poor charge

transport, but exceptional mechanical properties. Studies have been performed on copolymers of 1:1 P3OT-*b*-P3HT (**2b**), resulting in a modulus (0.68 GPa) approximately halfway between the two homopolymers, while still providing a fully absorptive system.<sup>82</sup> This effect can be generalized, as the modulus of two moderately soluble polymers is expected to display a synergistic modulus.<sup>113</sup> Furthermore, OPV devices made with this copolymer exhibits a higher PCE (1.56%) than a linear extrapolation of properties between P3HT (**2b**) (2.04%) and P3OT (0.67%) would imply.<sup>82</sup>

When these copolymers are extended to triblock, or three component copolymers, the segregation of the system can generate properties similar to elastomers. These systems are commonly called thermoplastic elastomers. Thermoplastic elastomers form when two materials, one being rigid and the other elastic, self-assemble into crystalline domains of hard segment rich phases and soft segment rich phases. These hard segments then act as rigid crosslinks for the stretchable rubber segments, resulting in an extensibility that resembles a traditional thermoset material (Figure 13a). Given that many organic semiconductor materials are rigid, they can be input into block copolymers as a rigid segment and combined with a soft segment to generate block copolymers that phase segregate.<sup>114</sup> An example of this arrangement was shown using poly(methyl acrylate) (PMA) in a P3HT (**2b**)-*b*-PMA-*b*-P3HT (**2b**) triblock copolymer, diagrammed in Figure 13b. The phase segregation was confirmed by DSC, where distinct transitions for PMA and P3HT were observed. This phase segregation leads to thermoplastic elastomer-like properties, resulting in a maximum elongation of 140% with a composition of 35 wt% P3HT (**2b**). Interestingly, there was a net improvement in charge

transport when a small amount of PMA was added, due to induced ordering effects in the block copolymer. At lower concentrations, this effect is overridden by the resistivity of PMA. The mobility was permanently lowered after applying significant strains (>40%), and at 60% strain, the mobility was 10% that of the unstrained film.<sup>115</sup>

### Random copolymers

Random or statistical copolymers provide an opportunity to input a certain amount of each monomer into the final polymer, allowing for the tuning of material properties without introducing a multiphase system. Depending on the relative amounts of the two polymers, this can produce a polymer with approximately equivalent amounts of each component, or a segmented polymer, one that is mostly one component, with only small amounts of the minor component. The effect of segmentation has been examined in PDPP2FT (**9**) by introducing bithiophene units at a ratio of 5:1. In the neat film, the material had a modulus of 2.17 GPa, but after segmentation the material showed a dramatically lower modulus of 0.93 GPa. Note that this modulus is lower than either PDPP2FT (**9**) in its pure state, or a pure PT2T (**4**) (1.11 GPa). Although this significantly reduced the modulus, it had a minimal effect on electrical properties, resulting in nearly identical PCEs between pure PDPP2FT (**9**) and the segmented version.<sup>91</sup> Although this is only one data point, it demonstrates that the modulus can be lowered with minimal effect on PCE by segmentation.

The case of copolymers containing approximately equivalent, randomly distributed amounts of each polymer has also been investigated. A statistical copolymer of 3-hexylthiophene and 3-octylthiophene showed a significantly lower modulus than a simple linear interpolation of properties would predict. This disruption is noted irrespective of the crystal structure.<sup>82,91</sup> This excessive lowering of modulus is attributed to the randomness in packing of the side chains of the two materials, causing a disruption in the crystalline packing of the material. However, unlike the segmentation, this change results in lower electrical properties at a level predicted by a

linear mixture of the two materials.<sup>82</sup> Ultimately, it seems as though segmentation, rather than fully random copolymers, may provide a more versatile tool for mechanical modification.

### POLYMER BLENDS FOR ORGANIC ELECTRONICS

Blends excellently illustrate how two polymers of drastically different properties can be combined into one material with an electrical component from the conjugated polymer and high mechanical durability from the elastomer. Various techniques for synthesis and preparation of blends and composites have been explored.<sup>116–118</sup> Literature since the late 20th century is rich in examples of blends and composites containing conjugated polymers,<sup>119</sup> such as P3HT (**2b**)/polystyrene,<sup>120–122</sup> or PA (**1**)/PE<sup>123,124</sup> with the purpose of improving the mechanical stability of the conjugated polymer applications, namely field-effect transistors. The conducting polymer polyaniline (**3**), in particular, has been extensively studied in elastomer blends with rubbers including polyurethanes (PUs),<sup>125</sup> nitrile rubber,<sup>119,126,127</sup> polystyrene-*b*-poly(ethylene-*co*-butylene)-*b*-polystyrene<sup>128,129</sup> and others. To move forward in the improvement of both electrical and mechanical properties of stretchable electronics, it is necessary to understand how molecular interactions in blends and nanocomposites affect the material's performance.

Recent progress indicates a few general trends for such blends. Examples in Figure 14 clearly present that these blends do not simultaneously exhibit significant conductivity and high elongation at break. This can be explained by the morphology of these usually immiscible blends; larger domains of conjugated polymer improve electrical properties but introduce more of its brittle character as its concentration increases.<sup>125,130,131</sup> An example is illustrated in Figure 15, where larger phases of conducting polymer and higher miscibility between polymers showed increased conductivity.<sup>129</sup> To maintain conductivity without greatly changing the mechanical properties of the rubber, low percolation thresholds of conjugated polymers are desirable. It is continuously seen that the addition of insulator, even at low concentrations, improves electrical properties

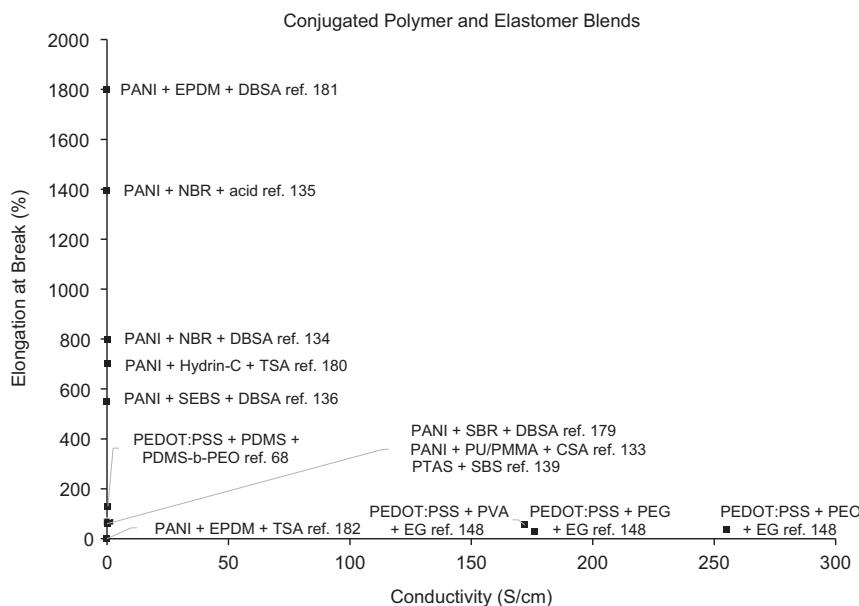


**Figure 14** Conjugated polymer/elastomer blends generally show a trend where either conductivity or elongation at break improves, but not both. CSA, camphor sulfonic acid; DBSA, dodecylbenzene sulfonic acid; EPDM, poly(ethylene-*co*-propylene-*co*-diene-monomer); Hydrin-C, poly(epichlorohydrin-*co*-ethylene oxide); NBR, nitrile rubber; PANI, polyaniline; PEG, polyethylene glycol; PEO, polyethyleneoxide; PTAS, poly(thiourea-azo-sulfone); TSA, *p*-toluene sulfonic acid.



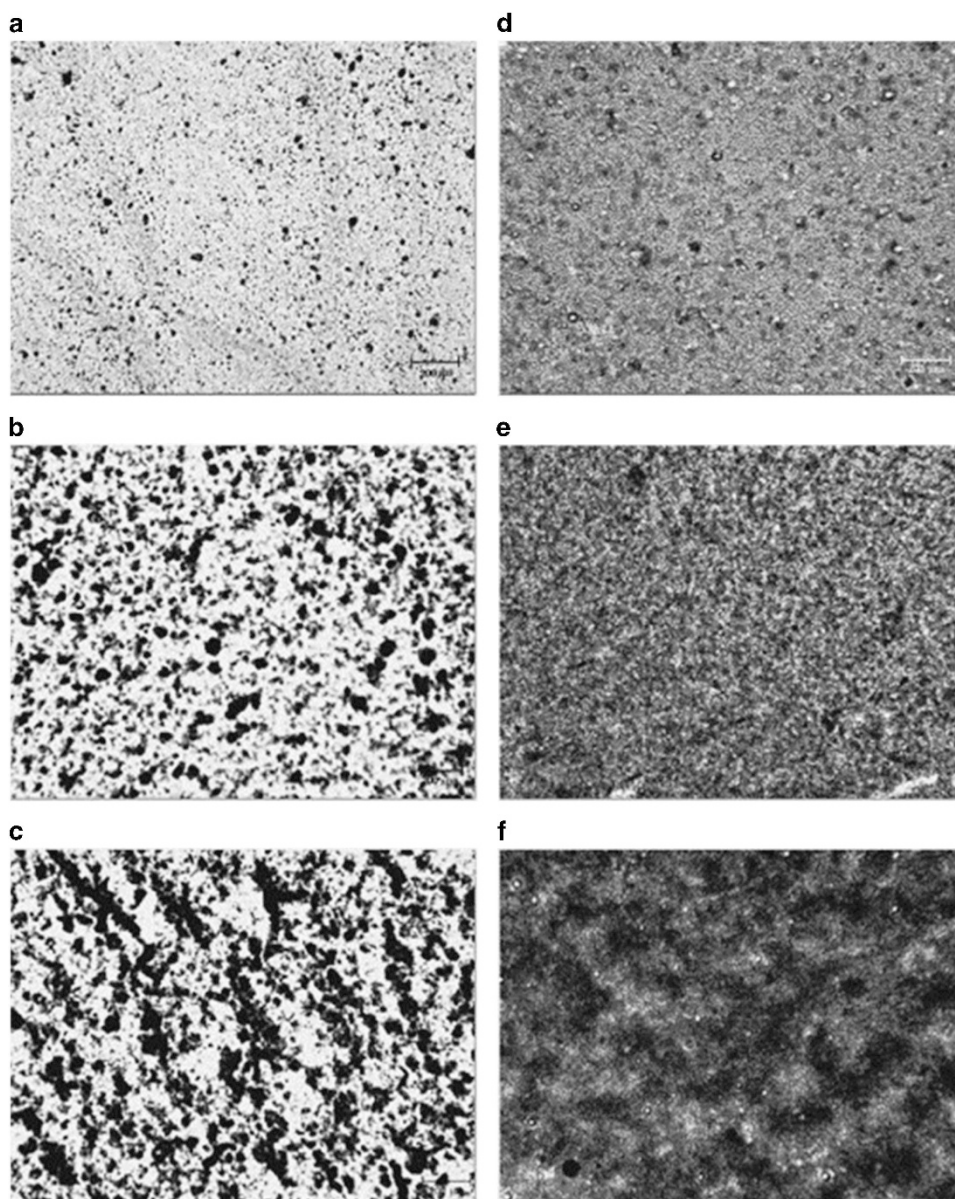


**Figure 15** Dark domains of increasing polyaniline (PANI) concentration 5%, 15%, 30% (a–c) in polystyrene-*b*-poly(ethylene-*co*-butylene)-*b*-polystyrene (SEBS) and (d–f) in sulfonated SEBS. Reproduced from Barra *et al.* with permission from Elsevier.<sup>129</sup>

compared with a pure conjugated polymer due to increased long-range order from polymer incompatibility. Temperature, pressure, composition and a few molecular parameters determine miscibility, and therefore affect morphology and performance in polymer blends.<sup>132</sup>

As represented in the following examples, we discuss stretchable conjugated polymer/elastomer blends where both electrical and mechanical properties were tested, and how these properties are affected by miscibility, nanostructure, chemical additives and preparation procedures.

#### Molecular mixing

Molecular mixing is defined as the formation of a single phase when two components are mixed together. Several experiments have been performed that indicate that improved molecular miscibility can improve the electrical and mechanical properties of a mixture. A suitable starting point for understanding a mixture's dependence

on composition is described by Fox's equation<sup>133</sup> and related equations.<sup>134</sup> However, these approximations apply only to homogeneous systems composed of similar polymers, and the detailed knowledge and structure–property relationships in dissimilar polymer blends require further examination.

Molecularly mixed PEDOT (**10**), and PU blends have achieved conductivity close to pure PEDOT (**10**).<sup>130</sup> The lack of phase segregation in the material was confirmed by AFM, and by DSC, which showed a mixing of the glass transitions, resulting in a  $T_g$  intermediate between the two components'  $T_g$ . This blend was conductively stable through four cycles of a high 200% strain.

Another example of molecularly mixed conjugated polymer and elastomer are PTAS (poly(thiourea-azo-sulfone) (**13**)) and SBS (poly(styrene-butadiene-styrene)).<sup>131</sup> The single phase morphology of the PTAS (**13**) and SBS film was confirmed by SEM. Though the conductivity of PTAS (**13**) decreased from  $2.42 \text{ S cm}^{-1}$  to  $0.065\text{--}1.43 \text{ S cm}^{-1}$  in the blends, the mechanical properties improved



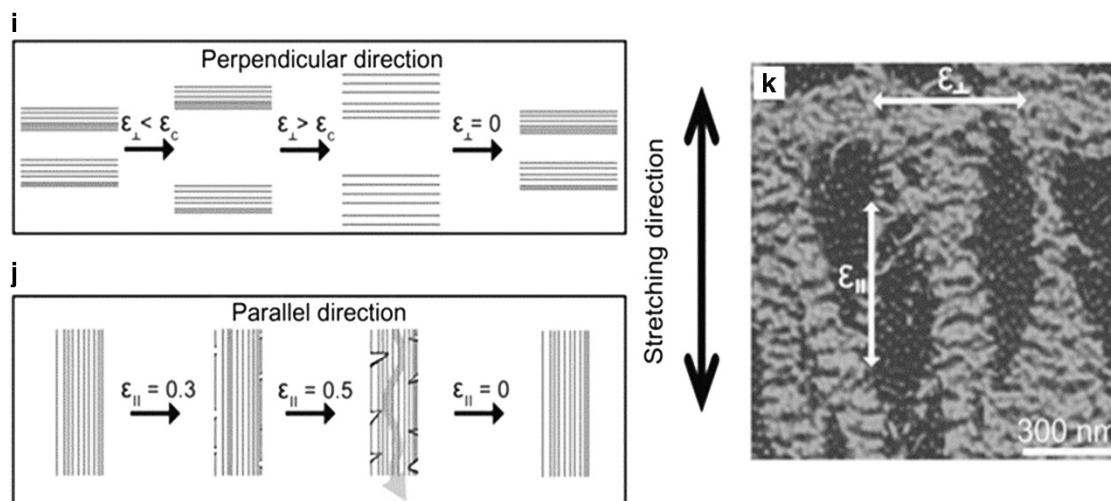


**Figure 16** Image i shows that stretching perpendicular to nanofibril orientation spreads nanofibrils further apart, resulting in no damage. Image j shows parallel stretching pulls the nanofibrils in tension, breaking the conjugated domains in the nanofibrils, resulting in greatest decrease in electrical performance. Image k is an AFM image that illustrates the different nanofibril orientations, and the relative directions of applied strain. Reproduced from Shin *et al.*<sup>136</sup> with permission from John Wiley & Sons, Inc.

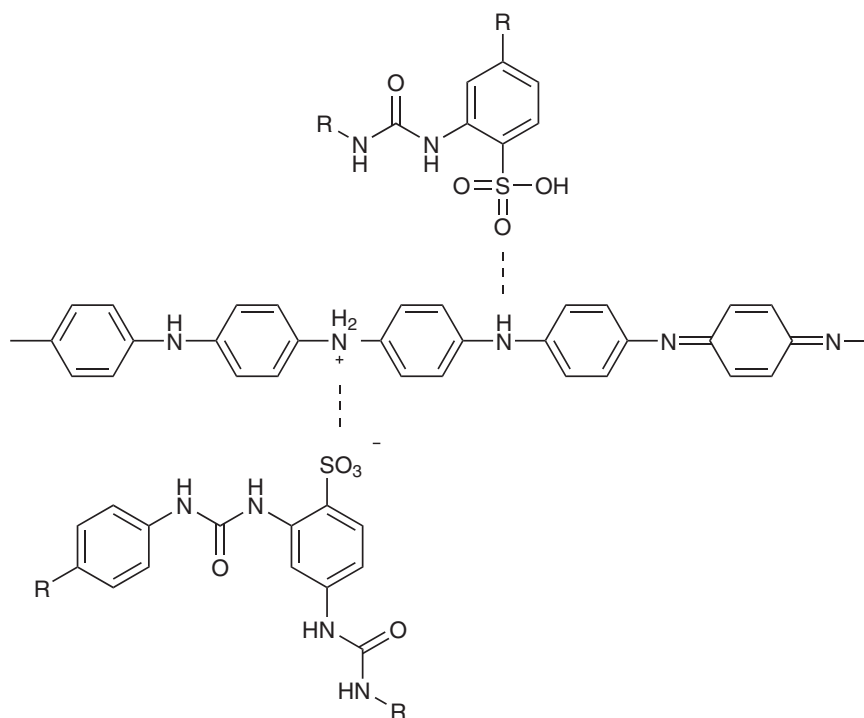


**Figure 17** Sulfonated polyurethane (PU) has both ionic and H-bonding interaction with doped polyaniline (PANI) to encourage molecular mixing. Redrawn from an original illustration in Ho *et al.*<sup>116</sup>

with higher PTAS (**13**) content, contrary to phase-segregated blends. This is attributed to the stronger intermolecular interactions between the two different polymers. Further studies are required to understand the mechanisms of these intermolecular interactions and phase formations as well as their effects on mechanical properties.

### Nanocomposites

Instead of blending molecular components together, a matrix can also be blended with a semiconducting nanoparticle to provide efficient charge transport pathways in a non-conducting matrix. The

incorporation of P3HT (**2b**) nanowires in PDMS showed equivalent mobility to pure P3HT (**2b**) nanowires. However, when stretched above 50% strain, the composite showed better properties than strained pure nanowires.<sup>135</sup> The maintained field-effect mobility of the composite at high strains can be attributed to greater freedom of motion for the nanowires inside the PDMS matrix rather than in the pure nanowire crystal superstructure, allowing rotation of the wires, dissipating strain.

An interesting element of another P3HT (**2b**) nanocomposites is the anisotropy of mechanical response. Specifically, the material had

significantly different response to strain depending on the direction of strain with respect to the orientation of the conjugated polymer network.<sup>136</sup> It was preferential for nanofibrils to align perpendicularly to the strain direction because stretching simply spaces fibrils further apart, whereas parallel stretching puts strain directly on the strands, leading to breakage of the nanofibrils, which diminishes electrical properties (Figure 16). Strains oriented perpendicular to the nanowires allowed for 200 cycles at 50% strain without completely suppressing conductivity.

#### Additives and modifiers

Additives can have a significant role in determining the properties of conjugated polymer/elastomer blends. Phase-inducing additives such as dimethyl sulfoxide,<sup>137,138</sup> ethylene glycol<sup>139,140</sup> and fluorosurfactants<sup>141,142</sup> are known to improve electrical properties by creating larger domains for charge transport. Insulating additives such as block copolymer surfactants<sup>60</sup> and crosslinking agents,<sup>126</sup> lower electrical performance. Large sulfonated acids are common dopants that are also used to solubilize more polar molecules in organic solvents.<sup>127,143</sup> Discussed here are a surfactant, chain extender, phase-inducer and plasticizer.

By adding a block copolymer of PEDOT (10) and polyethyleneoxide, a surfactant, PEDOT:PSS (10:11) and PDMS can be made macroscopically miscible.<sup>60</sup> The sheet resistance with a 30% surfactant concentration (200–300 Ohm/sq) lay between the pure PDMS ( $10^7$  Ohm sq<sup>-1</sup>) and PEDOT:PSS (10:11) (0.9–1.1 ohm sq<sup>-1</sup>) and the modulus and elongation at break of the blend, as expected, was inferior to pure PDMS (modulus 605 kPa; elongation at break 446%). By varying concentrations of rubber and PEDOT:PSS (10:11), sheet resistance and rupture point were found to be directly proportional, showing an inverse relationship between electrical and mechanical performance.

A blend of polyaniline (PANI) (3) with a sulfonic chain extender in PU, *m*-phenylene 4-diaminosulfonic acid, exhibited increased intermolecular H-bonding and ionic interaction with the assistance of an acidic dopant, leading to improved miscibility.<sup>125</sup> A depiction of this mechanism is shown in Figure 17. These strong ionic and H-bonding interactions improved conductivity and tensile strength by encouraging a higher degree of mixing similar to molecularly mixed examples above. Conversely, a chain extender with weaker conductor–insulator interactions and lower miscibility showed a decrease in tensile strength but increasing conductivity from larger conducting domains.

Another PEDOT:PSS (10:11) blend was tested with three insulating polymers—polyethylene glycol, polyethyleneoxide and poly(vinyl

alcohol).<sup>140</sup> The addition of polyethyleneoxide or polyethylene glycol increased the conductivity of PEDOT:PSS (10:11) from  $0.2 \text{ S cm}^{-1}$  to as high as  $101 \text{ S cm}^{-1}$  while decreasing the tensile strength and increasing the elongation at break. The highest conductivity in these blends was achieved with the addition of 3% polyethylene glycol, which induces phase segregation, to achieve conductivities up to  $255 \text{ S cm}^{-1}$  but slightly lowering the elongation at break. The H-bonding of poly(vinyl alcohol) to PEDOT increased the tensile strength and elongation at break, and decreased conductivity. In comparison with pure PEDOT:PSS (10:11), blends showed improved electrical and mechanical properties. However, alterations in the blends did not exhibit simultaneous improvement of both electrical and mechanical properties.

The addition of a plasticizer, Triton X-100,  $(\text{C}_{14}\text{H}_{22}\text{O}(\text{C}_2\text{H}_4\text{O})_n, n=9-10)$  completely transforms the brittle qualities of PEDOT:PSS (10:11) into a material with a dough-like consistency.<sup>144</sup> The plasticizer increases conductivity, forming nanofibrils of PEDOT (10) in the PSS (11)/plasticizer matrix. Though Triton X increases conductivity, and the dough exhibits mainly viscoelastic character rather than elastic. This is accompanied by a drastically reduced modulus, and an elasticity of only 10% strain, but 57% strain on a stretchable substrate. Conductivity in the dough is practically unchanged with 100 stretching cycles of 50% strain. Simply touching two cut pieces fully recovers initial current, which implied it can be used to treat connections in electrical equipment. Adhering plasticized PEDOT:PSS (10:11) to paper followed by crumpling, folding, twisting or spreading results in virtually no change in  $J-V$ , which demonstrates its potential for high deformation applications.

#### Processing and preparation

It is worth highlighting that the method chosen to prepare blends and composites can drastically affect the morphology and thus the final performance. Many methods have been explored to blend semiconducting polymers and insulating rubbers<sup>145,146</sup> but the majority fail to explore electrical–mechanical property relationships, which the next few examples discuss.

Mechanical and electrical properties of blends depend on the pre-deposition process—as is true for P3HT (2b) and PDMS blends.<sup>147</sup> These blends were prepared with and without sonication and the addition of poor solvent. Although PDMS predictably improved the mechanical properties of P3HT (2b), electrical properties improved as well. With the addition of insulating PDMS, improved charge transport pathways are formed which, because of the insolubility of P3HT (2b) and PDMS, forces P3HT (2b) to crystallize to larger self-assembled features to improve hole mobility. Phase segregation is

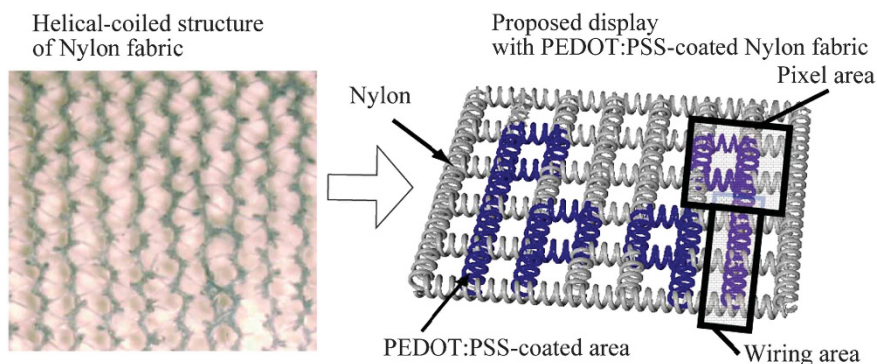


**Figure 18** Helical construction for stretchable conductive displays. Reproduced from Takamatsu with permission from IEEE.<sup>166</sup>

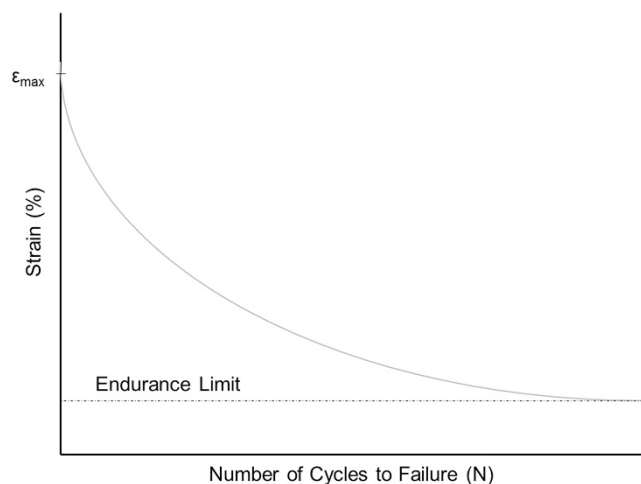


**Figure 19** A proposed 'electromechanical fatigue' curve is shown above. Note the exponential decay of the curve. Because of this behavior, these curves are sometimes depicted as strain vs  $\ln(N)$ , in which a linear curve is depicted.

further aided by sonication and the addition of poor solvent. Consequently, this lowered the crack-onset point, indicating that improvements in electrical properties simultaneously degraded mechanical properties.

In an experiment with PANI (3) and nitrile rubber, preparing blends by *in situ* polymerization produced different results from mechanically mixed samples of the same components.<sup>126</sup> Mechanically mixed PANI (3)/nitrile rubber exhibited agglomeration and low conductivity of  $10^{-4}$  to  $10^{-9}$  S  $\text{cm}^{-1}$ , whereas *in situ* polymerization of PANI (3) produced charge pathways. The protonating agent, dodecylbenzene sulfonic acid yielded a microtubular structure during emulsion, and resulted in two to four orders of magnitude higher conductivity. Both the samples showed increasing tensile strength and elongation at break compared with pure PANI (3), and a greater increase was observed in *in situ* samples.

## ENGINEERING AND DESIGN APPROACHES

Many reviews cover the design of silicon in stretchable electronics, including wavy ribbons,<sup>148</sup> pre-stained substrates,<sup>149</sup> mesh structures<sup>150</sup> or serpentine bridges<sup>151</sup> to provide mechanical flexibility and elasticity in electronics. Furthermore, carbon-based rubber fillers comprising of carbon black, carbon nanotubes and graphene have received much attention and reveal a promising future.<sup>152,153</sup> Engineering and design approaches are useful to a number of applications, particularly wearable sensors,<sup>154,155</sup> conductive textiles<sup>156,157</sup> and electronic skin.<sup>158,159</sup> Discussed are examples of engineering-based principles for conjugated polymers, which intentionally introduce physical features to relieve strain in the form of pre-stained substrates, coatings and fibers, to apply to various stretchable electrical devices.

### Pre-stained substrates

The pre-strain method has been proven successful for fabricating organic solar cells.<sup>160</sup> A wavy surface is formed by applying OPV layers onto a stretched PDMS substrate before relieving the strain. With pre-strains up to 27%, device performance did not heavily rely on the initial pre-strain, however the drawback to this method is that stretching must not exceed the initial pre-strain to prevent damage to the device from cracked brittle electrode and active layers. Though

electrical performance was not optimal, it served to prove that this technique makes stretchable solar cells possible.

The pre-strain approach has been improved with a fluorosurfactant, Zonyl ( $(\text{CF}_2\text{CF}_2)_x(\text{CH}_2\text{CH}_2\text{O})_y$ ), and dimethyl sulfoxide additives,<sup>141</sup> which induce phase segregation of PEDOT (10) and PSS (11) to reduce resistance 35% by increasing domain sizes, performing similar to those on ITO substrates (2.22% PCE) at 2.16% PCE. Pre-strained devices have also been tested with different substrate preparation methods. By treating substrates with ultraviolet and an ozone plasma,<sup>161</sup> electrode resistance increased less than 5% as opposed to  $\text{O}_2$  plasma, which drastically increased resistance by a factor of 10 000. The stability of these surface-treated devices was confirmed by completely reversible strain up to 30% with retained conductivity up to 188% strain. Variations on the pre-strain method illustrate viable results for stretchable photovoltaics.

### Coatings and fabrics

Free films of PU have been coated in polymer by soaking a PU film in a solution of 3-methylthiophene monomer and  $\text{FeCl}_3$  catalyst to polymerize a conductive surface layer.<sup>162</sup> Variables including monomer/rubber ratios, reaction time and catalyst concentration showed that improved conductivity and resistance came at the cost of reduced tensile strength and elongation at break, agreeing with electrical-mechanical property trends discussed earlier.

As the topic of stretchable electronics is receiving more attention, their application to textiles is also studied. Conductivity can be introduced by coating fiber with semiconducting polymers for applications like wearable electronics and displays. Woven photovoltaics with PEDOT:PSS (10:11) and P3HT (2b):PCBM (5) layers can be made on ITO the way textiles are processed in the die-coating method used to process textiles in industry.<sup>163</sup> Silver nanoparticle and multi-walled carbon nanotubes have been proven both stretchable and conductive when placed on a fabric of a tricot weave.<sup>164</sup> One coating method rolls organic device layers onto rubber tubes to make a conducting, stretchable yarn.<sup>165</sup> In another example, PEDOT:PSS (10:11) was coated on a fabric with a unique weave, pictured in Figure 18, such that the conductive coating on helical structures was not disturbed, but instead strain was accounted for by sections of the weave not coated by PEDOT:PSS (10:11).<sup>166</sup> At 125% strain, only a miniscule change in resistance was detected.

### Fibers

Fiber structures are an alternative method to relieve strain in a material. This is due to the presence of fewer internal defects compared with bulk material, resulting in effective uniaxial strength. Poly(styrene-isobutylene-styrene)/P3HT 2b fibers have been studied to create a material with a competitive combination of mechanical strain and conductivity.<sup>167</sup> At maximum strain, the resistance of these fibers after 20 cycles changed only 3%. It is suspected that resistance decreases after the 'threshold strain' because the isobutylene block of poly(styrene-isobutylene-styrene) undergoes strain-crystallization increasing contact between domains, increasing conductivity.

One example of composite fibers composed of semiconducting polymers and elastomer is with PANI (3) and natural rubber.<sup>168</sup> Through a wet-spinning processing technique, PANI (3) agglomerates were observed to mix inhomogeneously and preferentially cluster near the outer surface of fiber bundles. With increasing PANI (3) content, surface roughness and conductivity increased while tenacity (defined as a textile's breaking force per linear density) and elongation at breaking point decreased in comparison with natural rubber. Only a 5% PANI (3) content level produced conductivity, and it was virtually

unchanged in strains up to 600%. Doping predictably improved conductivity but further understanding as to why this also improves tenacity and elongation at break is to be investigated.

A recent article reports record conductivity in pure PEDOT:PSS (10:11) fibers.<sup>169</sup> A modified wet-spinning technique with a hot-drawing method provides high molecular alignment and creates semi-metallic microfibers with conductivity of  $2804 \text{ S cm}^{-1}$ . Spring-shaped fibers were stretchable to 257% elongation. Doping with ethylene glycol and de-doping (partial removal of PSS (11) by ethylene glycol) yielded the best electrical and mechanical properties, changing morphology from amorphous to small grains as more PSS was removed. Conductivity increases with strain, and remarkably with increased conductivity also came increased tensile strength, elongation at break and modulus.

## CONCLUSION

In homopolymers, the mechanical properties can be tuned using many methods. Increasing the stiffness of the molecular backbone, as well as the length and branching of the solubilizing side chains, can significantly alter the mechanical properties. In addition, increasing the molecular weight of the semiconducting polymer can improve both the mechanical properties and the PCE, while decreasing the regioregularity can improve mechanical properties, but lowers PCE. The formation of highly crystalline, nanometer-sized domains can result in exceptional PCE and mobility in homopolymer/PCBM blends, but this is usually at the expense of increased blend stiffness. The intercalation of PCBM to form co-crystalline domains also results in a significant increase in cohesion and stiffness, but also a reduction in PCE due to a lack of PCBM (5) percolation pathways; preventing PCBM intercalation can significantly improve both mechanical and electrical properties.

Using copolymer systems to improve the mechanical properties while maintaining charge mobility shows promise. Block copolymers have been shown to induce molecular ordering in semiconducting polymers, lowering the percolation percentage to as low as 10%, while improving the elongation at break to as high as 660%. Random copolymers can be used to 'segment' polymers, drastically lowering modulus while maintaining equivalent PCE to the pure homopolymer. The morphology and crystallinity of these structures has a significant effect, enabling significant extensibility through phase-segregated hard-soft-hard domains.

A general trend can be seen across different blends of conjugated and elastic polymers despite variation in materials and preparation methods. Although the addition of rubber improves electrical properties like conductivity, once a blend has been mixed, both electrical and mechanical properties are not simultaneously improved post-mixing. Future work should also consider elastomer properties such as gas permeability to ensure long lifetimes for sensitive active materials.<sup>170</sup> Polymer blends with good miscibility may improve both electrical and mechanical performance through stronger intermolecular interactions but further research is required. In-depth studies of morphology and phase separation will help scientists design materials of optimal electrical and mechanical properties from individual polymer properties.

Engineering solutions are important to stretchable electronics that use inorganic materials, and can be applied to conjugated polymer systems. There are several geometries that can provide admirable solutions, from pre-strained substrates to fibers. There are relatively few reports in the literature of polymer-based engineering solutions but these could provide interesting applications, such as functional clothing and stretchable displays. Although innovative design

approaches are a good way to alleviate material strain away from the conjugated polymer, it would be important to first fundamentally understand the contributing factors that each material brings to the final product before introducing more complicated device structures.

## OUTLOOK

In the field of organic stretchable electronics, in spite of the critical interplay between morphology and mechanical properties, very little data exists relating their electrical and mechanical properties. Ultimately the critical need is an expanded set of tested materials to allow for a systematic description of the effect of molecular design, crystallinity and morphology on the mechanical and electrical properties of a system.

As research of elastic electrical devices rapidly expands, it becomes increasingly important to set a standardized set of mechanical testing parameters to allow for easy comparison between different materials, as well as a complete description of the system. For these purposes, we suggest two test methods for electrical properties, two for mechanical properties and one for a quantitative comparative electromechanical test, for a total of five standard tests: (i) device resistance under zero strain; (ii) standard  $J$ - $V$  curve measurement; (iii) mechanical buckling test; (iv) measure of thin-film elongation at break; and (v) electro-mechanical fatigue test, modeled after fatigue testing (S-N Curves). The first four tests are already standard in the literature, while the fifth fatigue test, depicted in Figure 19, relates applied stress to a number of strain cycles, though with a limit on device resistance rather than mechanical failure. This test would be especially useful for quantifying the device's performance throughout operation, rather than only upon initial production.

To generate such a curve, a material is repeatedly cycled at different strains until each measures a certain value of resistance, such as 120% of the initial resistance. The number of cycles to achieve this given resistance is then recorded as  $N$ , the number of cycles to failure. The depicted exponential curve represents the typical behavior for an OPV. Of note is the 'Endurance Limit,' a line that defines a strain below which the device cannot fail, and can be cycled infinitely. Further, it would be of value to evaluate these data points against a set standard to give suitable quantitative data against particularly elastic, or particularly conductive systems, and deliver context for collected results.

## CONFLICT OF INTEREST

The authors declare no conflict of interest.

## ACKNOWLEDGEMENTS

We thank both Wesley Tatum and Sarah Holliday for their assistance in writing this paper. In addition, we gratefully acknowledge financial support from the NSF under DMR-1407815.

- Shirakawa, H., Louis, E. J., MacDiarmid, A. G., Chiang, C. K. & Heeger, A. J. Synthesis of electrically conducting organic polymers: halogen derivatives of polyacetylene, (CH)<sub>x</sub>. *J. Chem. Soc. Chem. Commun.* **474**, 578–580 (1977)
- Yip, H.-L. & Jen, A. K.-Y. Recent advances in solution-processed interfacial materials for efficient and stable polymer solar cells. *Energy Environ. Sci.* **5**, 5994–6011 (2012).
- Heumueeller, T., Mateker, W. R., Sachs-Quintana, I. T., Vandewal, K., Bartelt, J. A., Burke, T. M., Ameri, T., Brabec, C. J. & McGehee, M. D. Reducing burn-in voltage loss in polymer solar cells by increasing the polymer crystallinity. *Energy Environ. Sci.* **7**, 2974–2980 (2014).
- Joergensen, M., Norman, K. & Krebs, F. C. Stability/degradation of polymer solar cells. *Sol. Energy Mater. Sol. Cells* **92**, 714–786 (2008).



- 5 Jørgensen, M., Norman, K., Gevorgyan, S. A., Tromholt, T., Andreasen, B. & Krebs, F. C. Stability of polymer solar cells. *Adv. Mater.* **24**, 580–612 (2012).
- 6 Hwang, D. K., Fuentes-Hernandez, C., Fenoll, M., Yun, M., Park, J., Shim, J. W., Knauer, K. A., Dindar, A., Kim, H., Kim, Y., Kim, J., Cheun, H., Payne, M. M., Graham, S., Im, S., Anthony, J. E. & Kippelen, B. Systematic reliability study of top-gate p- and n-channel organic field-effect transistors. *ACS Appl. Mater. Interfaces* **6**, 3378–3386 (2014).
- 7 Liu, Y., Zhao, J., Li, Z., Mu, C., Ma, W., Hu, H., Jiang, K., Lin, H., Ade, H. & Yan, H. Aggregation and morphology control enables multiple cases of high-efficiency polymer solar cells. *Nat. Commun.* **5**, 5293 (2014).
- 8 You, J., Dou, L., Yoshimura, K., Kato, T., Ohya, K., Moriarty, T., Emery, K., Chen, C., Gao, J., Li, G. & Yang, Y. A polymer tandem solar cell with 10.6% power conversion efficiency. *Nat. Commun.* **4**, 1446 (2013).
- 9 Dou, L., You, J., Yang, J., Chen, C., He, Y., Murase, S., Moriarty, T., Emery, K., Li, G. & Yang, Y. Tandem polymer solar cells featuring a spectrally matched low-bandgap polymer. *Nat. Photonics* **6**, 180–185 (2012).
- 10 He, Z., Zhong, C., Su, S., Xu, M., Wu, H. & Cao, Y. Enhanced power-conversion efficiency in polymer solar cells using an inverted device structure. *Nat. Photonics* **6**, 593–597 (2012).
- 11 Scharber, M. C., Koppe, M., Gao, J., Cordella, F., Loi, M. A., Denk, P., Morana, M., Egelhaaf, H., Forberich, K., Dennler, G., Gaudiana, R., Waller, D., Zhu, Z., Shi, X. & Brabec, C. J. Influence of the bridging atom on the performance of a low-bandgap bulk heterojunction solar cell. *Adv. Mater.* **22**, 367–370 (2010).
- 12 Bharti, D. & Tiwari, S. P. Crystallinity and performance improvement in solution processed organic field-effect transistors due to structural dissimilarity of the additive solvent. *Synth. Met.* **215**, 1–6 (2016).
- 13 Yang, S. Y., Shin, K. & Park, C. E. The effect of gate-dielectric surface energy on pentacene morphology and organic field-effect transistor characteristics. *Adv. Funct. Mater.* **15**, 1806–1814 (2005).
- 14 Zhao, Y., Meeck, G. A., Levine, B. G. & Lunt, R. R. Near-infrared harvesting transparent luminescent solar concentrators. *Adv. Opt. Mater.* **2**, 606–611 (2014).
- 15 Brabec, C. J. & Durrant, J. R. Solution-processed organic solar cells. *MRS Bull.* **33**, 670–675 (2008).
- 16 Kaltenbrunner, M., White, M. S., Glowacki, E. D., Sekitani, T., Someya, T., Sariciftci, N. S. & Bauer, S. Ultrathin and lightweight organic solar cells with high flexibility. *Nat. Commun.* **3**, 770 (2012).
- 17 Krebs, F. C., Nielsen, T. D., Fyenbo, J., Wadstrøm, M. & Pedersen, M. S. Manufacture, integration and demonstration of polymer solar cells in a lamp for the 'Lighting Africa' initiative. *Energy Environ. Sci.* **3**, 512–522 (2010).
- 18 Grossiord, N., Kroon, J. M., Andriessen, R. & Blom, P. W. M. Degradation mechanisms in organic photovoltaic devices. *Org. Electron.* **13**, 432–456 (2012).
- 19 Sekitani, T., Nakajima, H., Maeda, H., Fukushima, T., Aida, T., Hata, K. & Someya, T. Stretchable active-matrix organic light-emitting diode display using printable elastic conductors. *Nat. Mater.* **8**, 494–499 (2009).
- 20 Sokolov, A. N., Cao, Y., Johnson, O. B. & Bao, Z. Mechanistic considerations of bending-strain effects within organic semiconductors on polymer dielectrics. *Adv. Funct. Mater.* **22**, 175–183 (2012).
- 21 Loi, A., Basiricò, L., Cosseddu, P., Lai, S., Barbaro, M., Bonfiglio, A., Maiolino, P., Baglini, E., Denei, S., Mastrogianni, F. & Cannata, G. Organic bendable and stretchable field effect devices for sensing applications. *IEEE Sens. J.* **13**, 4764–4772 (2013).
- 22 Yi, H. T., Payne, M. M., Anthony, J. E. & Podzorov, V. Ultra-flexible solution-processed organic field-effect transistors. *Nat. Commun.* **3**, 1259 (2012).
- 23 Bruner, C., Miller, N. C., McGehee, M. D. & Dauskardt, R. H. Molecular intercalation and cohesion of organic bulk heterojunction photovoltaic devices. *Adv. Funct. Mater.* **23**, 2863–2871 (2013).
- 24 Lipomi, D. J., Chong, H., Vosgueritchian, M., Mei, J. & Bao, Z. Toward mechanically robust and intrinsically stretchable organic solar cells: evolution of photovoltaic properties with tensile strain. *Sol. Energy Mater. Sol. Cells* **107**, 355–365 (2012).
- 25 Kim, B. J., Shin, H. A. S., Choi, I. S. & Joo, Y. C. Electrical failure and damage analysis of multi-layer metal films on flexible substrate during cyclic bending deformation in *Proc. Int. Symp. Vol. 18* (Physical and Failure Analysis of Integrated Circuits (IPFA), Incheon, South Korea, 2011).
- 26 Someya, T. *Stretchable Electronics* (Wiley-VCH, Weinheim, Germany, 2013).
- 27 Yao, Y., Dong, H. & Hu, W. Charge transport in organic and polymeric semiconductors for flexible and stretchable devices. *Adv. Mater.* **28**, 4213–4523 (2015).
- 28 Rogers, J. A., Someya, T. & Huang, Y. Materials and mechanics for stretchable electronics. *Science* **327**, 1603–1607 (2010).
- 29 Vosgueritchian, M., Tok, J. B.-H. & Bao, Z. Stretchable LEDs: light-emitting electronic skin. *Nat. Photonics* **7**, 769–771 (2013).
- 30 Savagatrup, S., Printz, A., O'Connor, T., Zaretski, A. & Lipomi, D. Molecularly stretchable electronics. *Chem. Mater.* **26**, 3028–3041 (2014).
- 31 ASTM B667-97. Standard Practice for Construction and Use of a Probe for Measuring Electrical Contact Resistance (ASTM International, West Conshohocken, PA, USA, 2014).
- 32 Brennan, R. & Dickey, D. Determination of diffusion characteristics using two- and four-point probe measurements. *Solid State Technol.* **27**, 125–132 (1984).
- 33 Smits, F. M. Measurement of sheet resistivities with the four-point probe. *Bell Syst. Tech. J.* **37**, 711–718 (1958).
- 34 Kippelen, B., Yoo, S., Haddock, J. A., Domercq, B., Barlow, S., Minch, B., Xia, W., Marder, S. R. & Armstrong, N. R. in *Organic Photovoltaics: Mechanisms Materials, and Devices* (eds Sun, S.-S. & Sariciftci, N. S.) Ch. 11, 271–298 (Taylor & Francis Group, Boca Raton, FL, USA, 2005).
- 35 Dost, R., Das, A. & Grell, M. Time-of-flight mobility measurements in organic field-effect transistors. *J. Appl. Phys.* **104**, 084519 (2008).
- 36 Chen, B., Lee, C., Lee, S., Webb, P., Chan, Y., Gambling, W., Tian, H. & Zhu, W. Improved time-of-flight technique for measuring carrier mobility in thin films of organic electroluminescent materials. *Jpn. J. Appl. Phys.* **39**, 1190–1192 (2000).
- 37 Mihaleitchi, V. D., Wildeman, J. & Blom, P. W. M. Space-charge limited photocurrent. *Phys. Rev. Lett.* **94**, 126602 (2005).
- 38 Yasuda, T., Yamaguchi, Y., Zou, D.-C. & Tsutsui, T. Carrier mobilities in organic electron transport materials determined from space charge limited current. *Jpn. J. Appl. Phys.* **41**, 5626–5629 (2002).
- 39 Saeki, A., Tsuji, M. & Seki, S. Direct evaluation of intrinsic optoelectronic performance of organic photovoltaic cells with minimizing impurity and degradation effects. *Adv. Energy Mater.* **1**, 661–669 (2011).
- 40 Yoshikawa, S., Saeki, A., Saito, M., Osaka, I. & Seki, S. On the role of local charge carrier mobility in the charge separation mechanism of organic photovoltaics. *Phys. Chem. Chem. Phys.* **17**, 17778–17784 (2015).
- 41 Gamota, D. & Paul Brazis, J. IEEE Standard for Test Methods for the Characterization of Organic Transistors and Materials. *IEEE Std 1620-2008* 1–14 (2008)
- 42 ASTM E772-15. Standard Terminology of Solar Energy Conversion (ASTM International, West Conshohocken, PA, USA, 2015).
- 43 ASTM E948-15. Standard Test Method for Electrical Performance of Photovoltaic Cells Using Reference Cells Under Simulated Sunlight (ASTM International, West Conshohocken, PA, USA, 2015).
- 44 ASTM D638-14. Standard Test Method for Tensile Properties of Plastics (ASTM International, West Conshohocken, PA, USA, 2014).
- 45 Gustafsson, G., Ingan, O., Stafstrom, S., Osterholm, H. & Laakso, J. Stretch-oriented poly(3-alkylthiophenes). *Synth. Met.* **41**, 593–596 (1991).
- 46 Moulton, J. & Smith, P. Electrical and mechanical properties of oriented poly(3-alkylthiophenes): 2. Effect of side-chain length. *Polymer* **33**, 2340–2347 (1992).
- 47 Ito, M., Tsuruno, A., Osawa, S. & Tanaka, K. Morphology and mechanical properties of electrochemically prepared polythiophene films. *Polymer* **29**, 1161–1165 (1988).
- 48 Chung, J. Y., Nolte, A. J. & Stafford, C. M. Surface wrinkling: a versatile platform for measuring thin-film properties. *Adv. Mater.* **23**, 349–368 (2011).
- 49 Bowden, N., Brittain, S. & Evans, A. Spontaneous formation of ordered structures in thin films of metals supported on an elastomeric polymer. *Nature* **393**, 146–149 (1998).
- 50 Bowden, N., Huck, W. T. S., Paul, K. E. & Whitesides, G. M. The controlled formation of ordered, sinusoidal structures by plasma oxidation of an elastomeric polymer. *Appl. Phys. Lett.* **75**, 2557–2559 (1999).
- 51 Savagatrup, S., Printz, A. D., O'Connor, T. F., Zaretski, A. V., Rodriguez, D., Sawyer, E. J., Rajan, K. M., Acosta, R. I., Root, S. E. & Lipomi, D. J. Mechanical degradation and stability of organic solar cells: molecular and microstructural determinants. *Energy Environ. Sci.* **8**, 55–80 (2014).
- 52 Khang, D., Rogers, J. A. & Lee, H. H. Mechanical buckling: mechanics, metrology, and stretchable electronics. *Adv. Funct. Mater.* **18**, 1–11 (2008).
- 53 O'Connor, T. F., Zaretski, A. V., Savagatrup, S., Printz, A. D., Wilkes, C. D., Diaz, M. I., Sawyer, E. J. & Lipomi, D. J. Wearable organic solar cells with high cyclic bending stability: Materials selection criteria. *Sol. Energy Mater. Sol. Cells* **144**, 438–444 (2016).
- 54 Savagatrup, S., Printz, A. D., Wu, H., Rajan, K. M., Sawyer, E. J., Zaretski, A. V., Bettinger, C. J. & Lipomi, D. J. Viability of stretchable poly(3-hexylthiophene) (P3HpT) for organic solar cells and field-effect transistors. *Synth. Met.* **203**, 208–214 (2015).
- 55 Jia, Z., Tucker, M. B. & Li, T. Failure mechanics of organic-inorganic multilayer permeation barriers in flexible electronics. *Compos. Sci. Technol.* **71**, 365–372 (2011).
- 56 Schnell, R., Stamm, M. & Creton, C. Direct correlation between interfacial width and adhesion in glassy polymers. *Macromolecules* **31**, 2284–2292 (1998).
- 57 Brown, H. Adhesion between polymers and other substances: a review of bonding mechanisms, systems and testing. *Azo Mater* **24**, 49–58 (2000).
- 58 Kaelble, D. H. Peel adhesion: influence of surface energies and adhesive rheology. *J. Adhes.* **1**, 102–123 (1969).
- 59 Creton, C., Hooker, J. & Shull, K. R. Bulk and interfacial contributions to the debonding mechanisms of soft adhesives: extension to large strains. *Langmuir* **17**, 4948–4954 (2001).
- 60 Noh, J.-S. Highly conductive and stretchable poly(dimethylsiloxane):poly(3,4-ethylenedioxythiophene):poly(styrene sulfonic acid) blends for organic interconnects. *RSC Adv.* **4**, 1857–1863 (2014).
- 61 Gladkov, S. O. & Nikol'skii, V. G. Multiple formation of microcracks during mechanical loading of polymers. *Tech. Phys. Lett.* **23**, 980–981 (1997).
- 62 Li, M., Li, H., Zhong, W., Zhao, Q. & Wang, D. Stretchable conductive polypyrrole/polyurethane (PPY/PU) strain sensor with netlike microcracks for human breath detection. *ACS Appl. Mater. Interfaces* **6**, 1313–1319 (2014).
- 63 Chen, J. Y., Kuo, C. C., Lai, C. S., Chen, W. C. & Chen, H. L. Manipulation on the morphology and electrical properties of aligned electrospun nanofibers of poly(3-hexylthiophene) for field-effect transistor applications. *Macromolecules* **44**, 2883–2892 (2011).
- 64 O'Connor, B., Kline, R. J., Conrad, B. R., Richter, L. J., Gundlach, D., Toney, M. F. & DeLongchamp, D. M. Anisotropic structure and charge transport in highly strain-aligned regioregular poly(3-hexylthiophene). *Adv. Funct. Mater.* **21**, 3697–3705 (2011).

- 65 Bradley, D. D. C. Precursor-route poly(p-phenylenevinylene): polymer characterisation and control of electronic properties. *J. Phys. D Appl. Phys.* **20**, 1389–1410 (1987).
- 66 Kim, K., Kim, J., Hyun, B. G., Ji, S., Kim, S., Kim, S., An, B. W. & Park, J. Stretchable and transparent electrodes based on in-plane structures. *Nanoscale* **7**, 14577–14594 (2015).
- 67 Chen, D., Liang, J. & Pei, Q. Flexible and stretchable electrodes for next generation polymer electronics: a review. *Sci. China Chem.* **59**, 659–671 (2016).
- 68 Cheng, T., Zhang, Y., Lai, W.-Y. & Huang, W. Stretchable thin-film electrodes for flexible electronics with high deformability and stretchability. *Adv. Mater.* **27**, 3349–3376 (2015).
- 69 O'Connor, B., Chan, E. P., Chan, C., Conrad, B. R., Richter, L. J., Kline, R. J., Heeney, M., McCulloch, I., Soles, C. L. & DeLongchamp, D. M. Correlations between mechanical and electrical properties of polythiophenes. *ACS Nano* **4**, 7538–7544 (2010).
- 70 Chen, L. M., Hong, Z., Li, G. & Yang, Y. Recent progress in polymer solar cells—manipulation of polymer: fullerene morphology and the formation of efficient inverted polymer solar cells. *Adv. Mater.* **21**, 1434–1449 (2009).
- 71 McNeill, C. R. Morphology of all-polymer solar cells. *Energy Environ. Sci.* **5**, 5653 (2012).
- 72 Gebeyehu, D., Brabec, C. J., Padinger, F., Fromherz, T., Hummelen, J. C., Badt, D., Schindler, H. & Sariciftci, N. S. Interplay of efficiency and morphology in photovoltaic devices based on interpenetrating networks of conjugated polymers with fullerenes. *Synth. Met.* **118**, 1–9 (2001).
- 73 Steyrlleuthner, R., Schubert, M., Jaiser, F., Blakesley, J. C., Chen, Z., Facchetti, A. & Neher, D. Bulk electron transport and charge injection in a high mobility n-type semiconducting polymer. *Adv. Mater.* **22**, 2799–2803 (2010).
- 74 Huang, W., Gann, E., Cheng, Y. B. & McNeill, C. R. In-depth understanding of the morphology-performance relationship in polymer solar cells. *ACS Appl. Mater. Interfaces* **7**, 14026–14034 (2015).
- 75 Zhao, B., Awtarani, O., O'Connor, B. & Zikry, M. A. Microstructural behavior and failure mechanisms of organic semicrystalline thin film blends. *J. Polym. Sci. Part B Polym. Phys.* **54**, 896–907 (2016).
- 76 Mei, J. & Bao, Z. Side chain engineering in solution-processable conjugated polymers. *Chem. Mater.* **26**, 604–615 (2014).
- 77 O'Connor, T. F., Zaretski, A. V., Shiravi, B. A., Savagatrup, S., Printz, A. D., Diaz, M. I. & Lipomi, D. J. Stretching and conformational bonding of organic solar cells to hemispherical surfaces. *Energy Environ. Sci.* **7**, 370–378 (2014).
- 78 Savagatrup, S., Makaram, A. S., Burke, D. J. & Lipomi, D. J. Mechanical properties of conjugated polymers and polymer-fullerene composites as a function of molecular structure. *Adv. Funct. Mater.* **24**, 1169–1181 (2014).
- 79 Pascui, O. F., Lohwasser, R., Sommer, M., Thelakkat, M., Thurn-Albrecht, T. & Saalwächter, K. High crystallinity and nature of crystal-crystal phase transformations in regioregular poly(3-hexylthiophene). *Macromolecules* **43**, 9401–9410 (2010).
- 80 Ren, G., Wu, P.-T. & Jenekhe, S. A. Enhanced performance of bulk heterojunction solar cells using block copoly(3-alkylthiophene)s. *Chem. Mater.* **22**, 2020–2026 (2010).
- 81 Sundberg, M., Inghan, O., Stafstrom, S., Gustafsson, G. & Sjogren, B. Optical absorption of poly(3-alkylthiophene) at low temperatures. *Solid State Commun.* **71**, 435–439 (1989).
- 82 Savagatrup, S., Printz, A. D., Rodriguez, D. & Lipomi, D. J. Best of both worlds: Conjugated polymers exhibiting good photovoltaic behavior and high tensile elasticity. *Macromolecules* **47**, 1981–1992 (2014).
- 83 Ho, V., Boudouris, B. W. & Segalman, R. A. Tuning polythiophene crystallization through systematic side chain functionalization. *Macromolecules* **43**, 7895–7899 (2010).
- 84 Yiu, A. T., Beaujuge, P. M., Lee, O. P., Woo, C. H., Toney, M. F. & Fréchet, J. M. Side-chain tunability of furan-containing low-band-gap polymers provides control of structural order in efficient solar cells. *J. Am. Chem. Soc.* **134**, 2180–2185 (2012).
- 85 Hopkinson, P. E., Staniec, P. A., Pearson, A. J., Dunbar, A. D. F., Wang, T., Ryan, A. J., Jones, R. A. L., Lidzey, D. G. & Donald, A. M. A phase diagram of the P3HT:PCBM organic photovoltaic system: Implications for device processing and performance. *Macromolecules* **44**, 2908–2917 (2011).
- 86 Deb, N., Li, B., Skoda, M., Rogers, S., Sun, Y., Gong, X., Karim, A., Sumpster, B. G. & Bucknall, D. G. Harnessing structure-property relationships for poly(alkyl thiophene)-fullerene derivative thin films to optimize performance in photovoltaic devices. *Adv. Funct. Mater.* **26**, 1908–1920 (2016).
- 87 Miller, N. C., Cho, E., Gysel, R., Risko, C., Coropceanu, V., Miller, C. E., Sweetnam, S., Sellinger, A., Heeney, M., McCulloch, I., Brédas, J., Toney, M. F. & McGehee, M. D. Factors governing intercalation of fullerenes and other small molecules between the side chains of semiconducting polymers used in solar cells. *Adv. Energy Mater.* **2**, 1208–1217 (2012).
- 88 McGehee, M. D., Cates, N. C., Gysel, R., Dahl, J. E. P. & Sellinger, A. Effects of intercalation on the hole mobility of amorphous semiconducting polymer blends. *Chem. Mater.* **22**, 3543–3548 (2010).
- 89 Cates, N. C., Gysel, R., Beiley, Z., Miller, C. E., Toney, M. F., Heeney, M., McCulloch, I. & McGehee, M. D. Tuning the properties of polymer bulk heterojunction solar cells by adjusting fullerene size to control intercalation. *Nano Lett.* **9**, 4153–4157 (2009).
- 90 Magnoni, M. C., Gallazzi, M. C. & Zerbi, G. Search for conducting doped polymers with great chemical stability: regiospecific poly(3,3'-dihexyl-2,2':5',2''-terthiophene). *Acta Polym.* **47**, 228–233 (1996).
- 91 Printz, A. D., Savagatrup, S., Burke, D. J., Purdy, T. N. & Lipomi, D. J. Increased elasticity of a low-bandgap conjugated copolymer by random segmentation for mechanically robust solar cells. *RSC Adv.* **4**, 13635–13643 (2014).
- 92 Koppe, M., Scharber, M., Brabec, C., Duffy, W., Heeney, M. & McCulloch, I. Polyterthiophenes as donors for polymer solar cells. *Adv. Funct. Mater.* **17**, 1371–1376 (2007).
- 93 Khang, D. Y., Rogers, J. A. & Lee, H. H. Mechanical buckling: mechanics, metrology, and stretchable electronics. *Adv. Funct. Mater.* **19**, 1526–1536 (2009).
- 94 Mayer, A. C., Toney, M. F., Scully, S. R., Rivnay, J., Brabec, C. J., Scharber, M., Koppe, M., Heeney, M., McCulloch, I. & McGehee, M. D. Bimolecular crystals of fullerenes in conjugated polymers and the implications of molecular mixing for solar cells. *Adv. Funct. Mater.* **19**, 1173–1179 (2009).
- 95 Parmer, J. E., Mayer, A. C., Hardin, B. E., Scully, S. R., McGehee, M. D., Heeney, M. & McCulloch, I. Organic bulk heterojunction solar cells using poly(2,5-bis(3-tetradecylthiophen-2-yl)thieno[3,2-b]thiophene). *Appl. Phys. Lett.* **92**, 113309 (2008).
- 96 Cheremisinoff, N. P. *Handbook of Polymer Science and Technology* (Marcel Dekker, Inc., New York, NY, USA, 1989).
- 97 Roth, B., Savagatrup, S., De Los Santos, N. V., Hagemann, O., Carle, J. E., Helgesen, M., Livi, F., Bundgaard, E., Sondergaard, R. R., Krebs, F. C. & Lipomi, D. J. Mechanical properties of a library of low-band-gap polymers. *Chem. Mater.* **28**, 2363–2373 (2016).
- 98 Tahk, D., Lee, H. H. & Khang, D. Y. Elastic moduli of organic electronic materials by the buckling method. *Macromolecules* **42**, 7079–7083 (2009).
- 99 Arnold, F. E. & Van Deusen, R. L. Preparation and properties of high molecular weight, soluble oxobenz[de]imidazobenzimidazoisquinoline ladder polymer. *Macromolecules* **2**, 497–502 (1969).
- 100 Nunes, R. W., Martin, J. R. & Johnson, J. F. Influence of molecular weight and molecular weight distribution on mechanical properties of polymers. *Polym. Eng. Sci.* **22**, 205–228 (1982).
- 101 Kang, H., Uddin, M. A., Lee, C., Kim, K. H., Nguyen, T. L., Lee, W., Li, Y., Wang, C., Woo, H. Y. & Kim, B. J. Determining the role of polymer molecular weight for high-performance all-polymer solar cells: Its effect on polymer aggregation and phase separation. *J. Am. Chem. Soc.* **137**, 2359–2365 (2015).
- 102 Tummala, N. R., Risko, C., Bruner, C., Dauskardt, R. H. & Brédas, J. L. Entanglements in P3HT and their influence on thin-film mechanical properties: Insights from molecular dynamics simulations. *J. Polym. Sci. Part B Polym. Phys.* **53**, 934–942 (2015).
- 103 Bruner, C. & Dauskardt, R. Role of molecular weight on the mechanical device properties of organic polymer solar cells. *Macromolecules* **47**, 1117–1121 (2014).
- 104 Mazzi, K. A., Rice, A. H., Durban, M. M. & Luscombe, C. K. Effect of regioregularity on charge transport and structural and excitonic coherence in poly(3-hexylthiophene) nanowires. *J. Phys. Chem. C* **119**, 14911–14918 (2015).
- 105 Kim, Y., Cook, S., Tuladhar, S. M., Choulis, S. A., Nelson, J., Durrant, J. R., Bradley, D. D. C., Giles, M., McCulloch, I., Ha, C.-S. & Ree, M. A strong regioregularity effect in self-organizing conjugated polymer films and high-efficiency polythiophene: fullerene solar cells. *Nat. Mater.* **5**, 197–203 (2006).
- 106 Woo, C. H., Thompson, B. C., Kim, B. J., Toney, M. F. & Fréchet, J. M. J. The influence of poly(3-hexylthiophene) regioregularity on fullerene-composite solar cell performance. *J. Am. Chem. Soc.* **130**, 16324–16329 (2008).
- 107 Kim, J. S., Kim, J. H., Lee, W., Yu, H., Kim, H. J., Song, I., Shin, M., Oh, J. H., Jeong, U., Kim, T. S. & Kim, B. J. Tuning mechanical and optoelectrical properties of poly(3-hexylthiophene) through systematic regioregularity control. *Macromolecules* **48**, 4339–4346 (2015).
- 108 Ghosh, S., Mishra, M. K., Kadambi, S. B., Ramamurty, U. & Desiraju, G. R. Designing elastic organic crystals: highly flexible polyhalogenated N-benzylideneanilines. *Angew. Chem. Int. Ed.* **54**, 2674–2678 (2015).
- 109 Reddy, C. M., Padmanabhan, K. A. & Desiraju, G. R. Structure-property correlations in bending and brittle organic crystals. *Cryst. Growth Des.* **6**, 2720–2731 (2006).
- 110 Miyane, S., Mori, H. & Higashihara, T. Synthesis and characterization of all-conjugated hard-soft-hard ABA triblock copolythiophenes. *Microsyst. Technol.* **22**, 3–10 (2016).
- 111 Iovu, M. C., Jeffries-El, M., Sheina, E. E., Cooper, J. R. & McCullough, R. D. Regioregular poly(3-alkylthiophene) conducting block copolymers. *Polymer* **46**, 8582–8586 (2005).
- 112 Müller, C., Goffri, S., Breiby, D. W., Andreasen, J. W., Chanzy, H. D., Janssen, R. A. J., Nielsen, M. M., Radano, C. P., Siringhaus, H., Smith, P. & Stingelin-Stutzmann, N. Tough, semiconducting polyethylene-poly(3-hexylthiophene) diblock copolymers. *Adv. Funct. Mater.* **17**, 2674–2679 (2007).
- 113 Hara, M. & Sauer, J. A. Synergism in mechanical properties of polymer/polymer blends. *J. Macromol. Sci. Part C Polym. Rev.* **38**, 327–362 (1998).
- 114 Radano, C. P., Scherman, O. A., Stingelin-Stutzmann, N., Müller, C., Breiby, D. W., Smith, P., Janssen, R. A. J. & Meijer, E. W. Crystalline-crystalline block copolymers of regioregular poly(3-hexylthiophene) and polyethylene by ring-opening metathesis polymerization. *J. Am. Chem. Soc.* **127**, 12502–12503 (2005).
- 115 Peng, R., Bo, P., Daqing, H., Mengjie, C., Guobing, Z., Xianghua, W., Hongbo, L., Kilwon, C. & Longzhen, Q. An ABA triblock copolymer strategy for intrinsically stretchable semiconductors. *J. Mater. Chem. C* **3**, 3599–3606 (2015).
- 116 Ho, K. S., Hsieh, K. H., Huang, S. K. & Hsieh, T. H. Polyurethane-based conducting polymer blends. I. Effect of chain extended. *Synth. Met.* **107**, 65–73 (1999).
- 117 De Paoli, M.-A. & Gazotti, W. A. Conductive polymer blends: preparation, properties and applications. *Macromol. Symp.* **189**, 83–104 (2002).

- 118 Anand, J., Palaniappan, S. & Sathyanarayana, D. Conducting polyaniline blends and composites. *Prog. Polym. Sci.* **23**, 993–1018 (1998).
- 119 Gomes de Souza, F., Almeida, M., Soares, B. G. & Carlos Pinto, J. Preparation of a semi-conductive thermoplastic elastomer vulcanizate based on EVA and NBR blends with polyaniline. *Polym. Test.* **26**, 692–697 (2007).
- 120 Han, S., Yu, X., Shi, W., Zhuang, X. & Yu, J. Solvent-dependent electrical properties improvement of organic field-effect transistor based on disordered conjugated polymer/insulator blends. *Org. Electron.* **27**, 160–166 (2015).
- 121 Qiu, L., Wang, X., Lee, W. H., Lim, J. A., Kim, J. S., Kwak, D. & Cho, K. Organic thin-film transistors based on blends of poly(3-hexylthiophene) and polystyrene with a solubility-induced low percolation threshold. *Chem. Mater.* **21**, 4380–4386 (2009).
- 122 Lu, G., Blakesley, J., Himmelberger, S., Pingel, P., Frisch, J., Lieberwirth, I., Salzmann, I., Oehzelt, M., Di Pietro, R., Salleo, A., Koch, N. & Neher, D. Moderate doping leads to high performance of semiconductor/insulator polymer blend transistors. *Nat. Commun.* **4**, 1588 (2013).
- 123 Dalton, L. R., Thomann, H., Morrobel-Sosa, A., Chiu, C., Galvin, M. E., Wnek, G. E., Tomkiewicz, Y., Shiren, N. S., Robinson, B. H. & Kwiram, A. L. Study of polyacetylene and composites of polyacetylene/polyethylene by electron nuclear double resonance, electron nuclear nuclear triple resonance, and electron spin echo spectroscopies. *J. Appl. Phys.* **54**, 5583–5591 (1983).
- 124 Galvin, M. E. & Wnek, G. E. Electrically conductive polymer composites: Polymerization of acetylene in polyethylene. *Polymer* **23**, 795–797 (1982).
- 125 Jeevananda, T. & Siddaramaiah Synthesis and characterization of polyaniline filled PU/PMMA interpenetrating polymer networks. *Eur. Polym. J.* **39**, 569–578 (2003).
- 126 Soares, B. G., Amorim, G. S., Oliveira, M. G. & Pereira Da Silva, J. E. Conducting elastomer blends based on nitrile rubber and pani.DBSA. *Macromol. Symp.* **233**, 95–101 (2006).
- 127 Vallim, M. R., Felisberti, M. I. & De Paoli, M. A. Blends of polyaniline with nitrile rubber. *J. Appl. Polym. Sci.* **75**, 677–684 (2000).
- 128 Barra, G. M. O., Matins, R. R., Kafer, K. A., Paniago, R., Vasques, C. T. & Pires, A. T. N. Thermoplastic elastomer/polyaniline blends: evaluation of mechanical and electromechanical properties. *Polym. Test.* **27**, 886–892 (2008).
- 129 Barra, G. M. O., Jacques, L. B., Orefice, R. L. & Carneiro, J. R. G. Processing, characterization and properties of conducting polyaniline-sulfonated SEBS block copolymers. *Eur. Polym. J.* **40**, 2017–2023 (2004).
- 130 Hansen, T. S., West, K., Hassager, O. & Larsen, N. B. Highly stretchable and conductive polymer material made from poly(3,4-ethylenedioxythiophene) and polyurethane elastomers. *Adv. Funct. Mater.* **17**, 3069–3073 (2007).
- 131 Kausar, A. Design, synthesis and physical properties of poly(styrene-butadiene-styrene)/poly(thiourea-azo-sulfone) blends. *Bull. Mater. Sci.* **37**, 917–923 (2014).
- 132 Takala, A., Takala, P., Seppala, J. & Levon, K. Interdiffusion and spinodal decomposition in electrically conducting polymer blends. *Polymers* **7**, 1410–1426 (2015).
- 133 Fox, T. G. & Flory, P. J. Second-order transition temperatures and related properties of polystyrene. I. Influence of molecular weight. *J. Appl. Phys.* **21**, 581 (1950).
- 134 Fried, J. R. *Polymer Science and Technology* 3rd edn (Prentice Hall, Westford, MA, USA, 2015).
- 135 Song, E., Kang, B., Choi, H. H., Sin, D. H., Lee, H., Lee, W. H. & Cho, K. Stretchable and transparent organic semiconducting thin film with conjugated polymer nanowires embedded in an elastomeric matrix. *Adv. Electron. Mater.* **2**, 1500250 (2016).
- 136 Shin, M., Oh, J. Y., Byun, K. E., Lee, Y. J., Kim, B., Baik, H. K., Park, J. J. & Jeong, U. Polythiophene nanofibril bundles surface-embedded in elastomer: a route to a highly stretchable active channel layer. *Adv. Mater.* **27**, 1255–1261 (2015).
- 137 Na, S.-I., Wang, G., Kim, S.-S., Kim, T.-W., Oh, S.-H., Yu, B.-K., Lee, T. & Kim, D.-Y. Evolution of nanomorphology and anisotropic conductivity in solvent-modified PEDOT: PSS films for polymeric anodes of polymer solar cells. *J. Mater. Chem.* **19**, 9045–9053 (2009).
- 138 Lee, I., Kim, G. W., Yang, M. & Kim, T. S. Simultaneously enhancing the cohesion and electrical conductivity of PEDOT:PSS conductive polymer films using DMSO additives. *ACS Appl. Mater. Interfaces* **8**, 302–310 (2016).
- 139 Lim, H. K., Lee, S. O., Song, K. J., Kim, S. G. & Kim, K. H. Synthesis and properties of soluble polypyrrole doped with dodecylbenzenesulfonate and combined with polymeric additive poly(ethylene glycol). *J. Appl. Polym. Sci.* **97**, 1170–1175 (2005).
- 140 Li, P., Sun, K. & Ouyang, J. Stretchable and conductive polymer films prepared by solution blending. *ACS Appl. Mater. Interfaces* **7**, 18415–18423 (2015).
- 141 Vosgueritchian, M., Lipomi, D. J. & Bao, Z. Highly conductive and transparent PEDOT: PSS films with a fluorosurfactant for stretchable and flexible transparent electrodes. *Adv. Funct. Mater.* **22**, 421–428 (2012).
- 142 Oh, J. Y., Shin, M., Lee, J. B., Ahn, J. H., Baik, H., Koo, J. & Jeong, U. Effect of PEDOT nanofibril networks on the conductivity, flexibility, and coatability of PEDOT:PSS films. *in ACS Appl. Mater. Interfaces* **6**, 6954–6961 (2014).
- 143 Cao, Y., Smith, P. & Heeger, A. J. Counter-ion induced processibility of conducting polyaniline and of conducting polyblends of polyaniline in bulk polymers. *Synth. Met.* **48**, 91–97 (1992).
- 144 Oh, J. Y., Kim, S., Baik, H. K. & Jeong, U. Conducting polymer dough for deformable electronics. *Adv. Mater.* **28**, 4455–4461 (2015).
- 145 Riaz, U. & Ashraf, S. M. *Nanostructured Polymer Blends* (eds Thomas, S., Shanks, R., & Sarathchandran, C.) Ch. 15, 509–538 (Elsevier, Waltham, MA, USA, 2014).
- 146 Njuguna, J. & Pielichowski, K. Recent developments in polyurethane-based conducting composites. *J. Mater. Sci.* **39**, 4081–4094 (2004).
- 147 Choi, D., Kim, H., Persson, N., Chu, P. H., Chang, M., Kang, J. H., Graham, S. & Reichmanis, E. Elastomer-polymer semiconductor blends for high-performance stretchable charge transport networks. *Chem. Mater.* **28**, 1196–1204 (2016).
- 148 Sun, Y., Choi, W. M., Jiang, H., Huang, Y. Y. & Rogers, J. A. Controlled buckling of semiconductor nanoribbons for stretchable electronics. *Nat. Nanotechnol.* **1**, 201–207 (2006).
- 149 Khang, D.-Y., Jiang, H., Huang, Y. & Rogers, J. A. A stretchable form of single-crystal silicon for high-performance electronics on rubber substrates. *Science* **311**, 208–212 (2006).
- 150 Kim, D.-H., Song, J., Choi, W. M., Kim, H.-S., Kim, R.-H., Liu, Z., Huang, Y. Y., Hwang, K.-C., Zhang, Y.-W. & Rogers, J. A. Materials and noncoplanar mesh designs for integrated circuits with linear elastic responses to extreme mechanical deformations. *Proc. Natl Acad. Sci. USA* **105**, 18675–18680 (2008).
- 151 Kim, D. H., Liu, Z., Kim, Y. S., Wu, J., Song, J. i., Kim, H. S., Huang, Y., Hwang, K. C., Zhang, Y. & Rogers, J. A. Optimized structural designs for stretchable silicon integrated circuits. *Small* **5**, 2841–2847 (2009).
- 152 Eccleston, W. Carbon as an electronics material. *J. Mater. Sci. Mater. Electron.* **17**, 399–404 (2006).
- 153 Avouris, P., Chen, Z. & Perebeinos, V. Carbon-based electronics. *Nat. Nanotechnol.* **2**, 605–615 (2007).
- 154 Trung, T. Q. & Lee, N. E. Flexible and stretchable physical sensor integrated platforms for wearable human-activity monitoring and personal healthcare. *Adv. Mater.* **28**, 4338–4372 (2016).
- 155 Brady, S., Lau, K. T., Megill, W., Wallace, G. G. & Diamond, D. The development and characterisation of conducting polymeric-based sensing devices. *Synth. Met.* **154**, 25–28 (2005).
- 156 Gregory, R. V., Kimbrell, W. C. & Kuhn, H. H. Conductive textiles. *Synth. Met.* **28**, 823–835 (1989).
- 157 Zeng, W., Shu, L., Li, Q., Chen, S., Wang, F. & Tao, X. M. Fiber-based wearable electronics: a review of materials, fabrication, devices, and applications. *Adv. Mater.* **26**, 5310–5336 (2014).
- 158 Ramuz, M., Tee, B. C. K., Tok, J. B. H. & Bao, Z. Transparent, optical, pressure-sensitive artificial skin for large-area stretchable electronics. *Adv. Mater.* **24**, 3223–3227 (2012).
- 159 Hammock, M. L., Chortos, A., Tee, B. C.-K., Tok, J. B.-H. & Bao, Z. 25th anniversary article: The evolution of electronic skin (E-Skin): a brief history, design considerations, and recent progress. *Adv. Mater.* **25**, 5997–6038 (2013).
- 160 Lipomi, D. J., Tee, B. C. K., Vosgueritchian, M. & Bao, Z. Stretchable organic solar cells. *Adv. Mater.* **23**, 1771–1775 (2011).
- 161 Lipomi, D. J., Lee, J., Vosgueritchian, M., Tee, B. C.-K., Bolander, J. & Bao, Z. Electronic properties of transparent conductive films of PEDOT:PSS on stretchable substrates. *Chem. Mater.* **24**, 373–382 (2012).
- 162 Ruckenstein, E. & Sun, Y. Synthesis of surface conductive polyurethane films. *Synth. Met.* **75**, 79–84 (1995).
- 163 Imai, T., Takamatsu, S., Shiraiishi, K., Marumoto, K. & Itoh, T. Photovoltaic textiles manufactured with precision die coating. *Procedia Eng.* **47**, 502–505 (2012).
- 164 Lee, Y. H., Kim, Y., Lee, T. I., Lee, I., Shin, J., Lee, H. S., Kim, T. S. & Choi, J. W. Anomalous stretchable conductivity using an engineered tricot weave. *ACS Nano* **9**, 12214–12223 (2015).
- 165 Takamatsu, S., Matsumoto, K. & Shimoyama, I. Stretchable yarn of display elements in *Proc. IEEE Int. Conf. Micro Electro Mech. Syst.* Vol 22, 1023–1026 (Sorrento, Italy, 2009).
- 166 Takamatsu, S., Matsumoto, K. & Shimoyama, I. Mechanically flexible and expandable display with conductive-polymer-coated nylon fabric in *Proc. IEEE Int. Conf. Micro Electro Mech. Syst.* Vol 21, 140–143 (Tucson, AZ, USA, 2008).
- 167 Granero, A. J., Wagner, P., Wagner, K., Razal, J. M., Wallace, G. G. & In Het Panhuis, M. Highly stretchable conducting SIBS-P3HT fibers. *Adv. Funct. Mater.* **21**, 955–962 (2011).
- 168 Sukitpaneenit, P., Thanpitcha, T., Sirivat, A., Weder, C. & Rujiravanit, R. Electrical conductivity and mechanical properties of polyaniline/natural rubber composite fibers. *J. Appl. Polym. Sci.* **106**, 4038–4046 (2007).
- 169 Zhou, J., Li, E. Q., Li, R., Xu, X., Ventura, I. A., Moussawi, A., Anjum, D. H., Hedhili, M. N., Smilgies, D.-M., Lubineau, G. & Thoroddsen, S. T. Semi-metallic, strong and stretchable wet-spun conjugated polymer microfibers. *J. Mater. Chem. C* **3**, 2528–2538 (2015).
- 170 Vohra, A., Filiatrault, H. L., Amyotte, S. D., Carmichael, R. S., Suhan, N. D., Siegers, C., Ferrari, L., Davidson, G. J. E. & Carmichael, T. B. Reinventing butyl rubber for stretchable electronics. *Adv. Funct. Mater.* **26**, 5222–5229 (2016).
- 171 Babel, A. & Jenekhe, S. A. Alkyl chain length dependence of the field-effect carrier mobility in regioregular poly(3-alkylthiophene)s. *Synth. Met.* **148**, 169–173 (2005).
- 172 Wu, P. T., Xin, H., Kim, F. S., Ren, G. & Jenekhe, S. A. Regioregular poly(3-pentylthiophene): Synthesis, self-assembly of nanowires, high-mobility field-effect transistors, and efficient photovoltaic cells. *Macromolecules* **42**, 8817–8826 (2009).
- 173 Tierney, S., Heaney, M. & McCulloch, L. Microwave-assisted synthesis of polythiophenes via the Stille coupling. *Synth. Met.* **148**, 195–198 (2005).
- 174 Chen, M. S., Lee, O. P., Niskala, J. R., Yiu, A. T., Tassone, C. J., Schmidt, K., Beaujeu, P. M., Onishi, S. S., Toney, M. F., Zettl, A. & Frechet, J. M. J. Enhanced solid-state order and field-effect hole mobility through control of nanoscale polymer aggregation. *J. Am. Chem. Soc.* **135**, 19229–19236 (2013).
- 175 Amorim, C. A., Cavallari, M. R., Santos, G., Fonseca, F. J., Andrade, A. M. & Mergulhao, S. Determination of carrier mobility in MEH-PPV thin-films by stationary and transient current techniques. *J. Non. Cryst. Solids* **358**, 484–491 (2012).



- 176 Patil, R., Harima, Y., Yamashita, K., Komaguchi, K., Itagaki, Y. & Shiotani, M. Charge carriers in polyaniline film: a correlation between mobility and in-situ ESR measurements. *J. Electroanal. Chem.* **518**, 13–19 (2002).
- 177 Von Hauff, E., Dyakonov, V. & Parisi, J. Study of field effect mobility in PCBM films and P3HT:PCBM blends. *Sol. Energy Mater. Sol. Cells* **87**, 149–156 (2005).
- 178 Babel, A. & Jenekhe, S. A. high electron mobility in ladder polymer field-effect transistors. *J. Am. Chem. Soc.* **125**, 13656–13657 (2003).
- 179 Martins, C. R., Faez, R., Rezende, M. C. & De Paoli, M. A. Reactive processing and evaluation of butadiene-styrene copolymer/polyaniline conductive blends. *J. Appl. Polym. Sci.* **101**, 681–685 (2006).
- 180 Gazotti, W. A., Faez, R. & De Paoli, M.-A. Thermal and mechanical behaviour of a conductive elastomeric blend based on a soluble polyaniline derivative. *Eur. Polym. J.* **35**, 35–40 (1999).
- 181 Domenech, S. C., Bortoluzzi, J. H., Soldi, V., Franco, C. V., Gronski, W. & Radosch, H.-J. Characterization, morphology, thermal and mechanical properties of conductive polyaniline-functionalized EPDM elastomers obtained by casting. *J. Polym. Sci. Part B Polym. Phys.* **42**, 1767–1782 (2004).
- 182 Faez, R., Gazotti, W. A. & De Paoli, M.-A. An elastomeric conductor based on polyaniline prepared by mechanical mixing. *Polymer* **40**, 5497–5503 (1999).



Jonathan Onorato received his BEng in Polymer Science and Engineering from Case Western Reserve University in 2015. There, his senior thesis research into dynamic covalent chemistry for the formation of network solids was performed under the direction of Professor Stuart Rowan. He is currently pursuing a PhD in Materials Science and Engineering at the University of Washington, where he received the Wagstaff Fellowship. He is currently working with Professor Christine Luscombe, investigating end-group modifications of semiconducting polymers to produce more mechanically durable polymers.



Viktoria Pakhnyuk received her BS in Chemistry from the University of Washington in 2014. She is a chemistry PhD student under the supervision of Professor Christine Luscombe at the University of Washington. Her current research investigates the development of mechanically stable polymeric materials for organic electronics.



Christine Luscombe received her BA, MSci, MA, and PhD degrees from the University of Cambridge (advisors: Prof. AB Holmes and Prof. WTS Huck), and then worked as a postdoctoral fellow at UC Berkeley (as a Lindemann Fellow), as well as a Trinity College Junior Research Fellow under the supervision of Prof. JMJ Frechet. In September 2006, she joined the Materials Science and Engineering Department at the University of Washington, Seattle. She received a number of young faculty awards including the NSF CAREER Award, DARPA Young Faculty Award, as well as the Sloan Research Fellowship. Her current research focuses on the synthesis of semiconducting polymers for energy applications. She is currently serving on the Editorial Advisory Boards for Polymer International, Advanced Electronic Materials, and Journal of Applied Physics. She is an Associate Editor for the Journal of Materials Chemistry A, is serving on the IUPAC Polymer Education and Polymer Terminology Subcommittees, and is the Vice President of the IUPAC Polymer Division.